Check for updates

ADVANCED MATERIALS
www.advmat.de

Micro-/Nanohierarchical Structures Physically Engineered on Surfaces: Analysis and Perspective

Junseong Ahn, Hyeonseok Han, Ji-Hwan Ha, Yongrok Jeong, Young Jung, Jungrak Choi, Seokjoo Cho, Sohee Jeon, Jun-Ho Jeong, and Inkyu Park**

The high demand for micro-/nanohierarchical structures as components of functional substrates, bioinspired devices, energy-related electronics, and chemical/physical transducers has inspired their in-depth studies and active development of the related fabrication techniques. In particular, significant progress has been achieved in hierarchical structures physically engineered on surfaces, which offer the advantages of wide-range material compatibility, design diversity, and mechanical stability, and numerous unique structures with important niche applications have been developed. This review categorizes the basic components of hierarchical structures physically engineered on surfaces according to function/shape and comprehensively summarizes the related advances, focusing on the fabrication strategies, ways of combining basic components, potential applications, and future research directions. Moreover, the physicochemical properties of hierarchical structures physically engineered on surfaces are compared based on the function of their basic components, which may help to avoid the bottlenecks of conventional single-scale functional substrates. Thus, the present work is expected to provide a useful reference for scientists working on multicomponent functional substrates and inspire further research in this field.

1. Introduction

Micro-/nanohierarchical structures physically engineered on surfaces have received significant attention and are in high demand owing to their utility in applications including contact angle manipulation,[1–6] bioinspired adhesives,[7–27] energy conversion/storage/harvesting devices,[28–30] and physical/chemical/biological sensors.[31–37] In addition, hierarchical structures have unique physicochemical properties originating from synergistic effects of constituent micro-/nanostructures.[38–41] These micro-/nanostructures are developed using various physical engineering methods such as casting, patterning by laser processing, nanowelding, patterning/wrinkling by mechanical deformation, spraying, thermal expansion/shrinkage, and imprinting. Then, hierarchical structures are constructed by combining two or more different structures with different scales (i.e., the scale of one component usually exceeds that of the other by one or more orders of magnitude)[19,21,42] or shapes (e.g., micropillars topped by microtips).[8,9,11,14,16,17,20,22] Although the individual components generally exhibit elevated specific surface area and roughness, based on their unique main function and shape, the building blocks of physically engineered hierarchical structures can be classified into five groups, namely rationally designed micropatterns, wrinkles, fibers, ordered nanopatterns, and random structures. Rationally designed micropatterns are used to tune substrate mechanical characteristics or impart the designed surface profile with uniformity (i.e., sample-to-sample variation),[43–50] while wrinkles can provide increased specific surface area and roughness with high robustness or stretchable highly dense curved structures.[51–53] Fibers (i.e., high-aspect-ratio pillars) are used to increase the active specific surface area and thus strengthen chemical reactions or van der Waals forces acting on the contact surface.[10,13,15,54,55] Ordered nanopatterns can provide increased nanoscale surface roughness for hydrophobicity/hydrophilicity tuning or unique nanophotonic properties such as structural color,[56,57] while random structures (e.g., random nanomaterials and microspheres) are mainly used to endow the surface with catalytic activity, chemical reactivity, or electrical conductivity and easily increase specific surface area and roughness.[30,58–60] Therefore, numerous functional substrates based on hierarchical structures can be realized by combining the abovementioned building blocks in various ways. For example, an integrated structure combining wrinkles and a random conductive nanomaterial exhibited high surface roughness together with high surface conductivity and was used to fabricate a high-performance triboelectric nanogenerator (TENG).[30] Gecko-inspired adhesives fabricated by combining micropatterns and fibers to achieve cumulative van der Waals interactions

J. Ahn, H. Han, J.-H. Ha, Y. Jeong, Y. Jung, J. Choi, S. Cho, I. Park
Department of Mechanical Engineering
Korea Advanced Institute of Science and Technology (KAIST)
Daejeon 34141, Republic of Korea
E-mail: inkyu@kaist.ac.kr

J. Ahn, J.-H. Ha, Y. Jeong, S. Jeon, J.-H. Jeong
Department of Nano Manufacturing Technology
Korea Institute of Machinery and Materials (KIMM)
Daejeon 34103, Republic of Korea
E-mail: jhjeong@kimm.re.kr

The ORCID identification number(s) for the author(s) of this article can be found under https://doi.org/10.1002/adma.202300871

DOI: 10.1002/adma.202300871

 © 2023 Wiley-VCH GmbH

Table 1. Types, materials, fabrication methods, functions, and limitations of the individual components of micro-/nanohierarchical structures physically engineered on surfaces.

Components	Fabrication methods (materials)	Main functions	Limitations
Rationally designed micropatterns	Casting process (PDMS,[66,67] Ecoflex,[67] Dragon Skin[68]) or micropatterning using photolithography[65]	Mechanical property tuning; formation of designed micropatterns	Low compatibility with soft substrates, low aspect ratio (e.g., 2D)
Wrinkles	Application of heat treatment to thermally shrinkable materials (PS[83]) Application of prestrain to stretchable substrates (PDMS,[93,94] Dragon Skin[62])	Provision of highly elevated specific surface area and roughness; highly dense stretchable curved structures[51–53]	Need for stretchable or thermally deformable substrates, low reliability and uniformity
Fibers	Imprinting using AAO templates,[10] physical transfer of fibers (CNTs),[15] and mechanical shear forces for fiber sealing[13]	Contact area increase for adhesion force enhancement; formation of nanoscale air gaps to achieve hydrophobicity	Low mechanical robustness
Random structures	Dry/wet etching,[117] thermally expandable microspheres,[116] laser patterning,[119] molding from naturally/artificially formed rough substrates[117]	Facile realization of surfaces with high catalytic activity, chemical reactivity, or electrical conductivity; increased specific surface area and roughness[30,58,59]	Low reliability, uniformity, and mechanical robustness
Ordered nanopatterns	Nanoimprinting lithography,[56] nanotransfer printing,[62] dry/wet etching[192]	Provision of increased nanoscale surface roughness for hydrophobicity/hydrophilicity tuning; realization of unique optical properties such as structural color[56,57]	Low design diversity, need for expensive equipment to fabricate master mold

showed high performance due to their large specific surface area and number of hairs (i.e., contact splitting principle)[55] as well as contact surface compliance caused by decreased structural stiffness coupled with mechanical stability.[10,15,61]

Hierarchical structures constructed by combining basic components feature a primary structure, which imparts or dramatically enhances the main function, and a secondary structure, which is combined with the primary structure to support the main function of the primary structure by obtaining synergistic effects. Thus, hierarchical structures can be categorized depending on the type of their main component (i.e., primary structure). This review categorizes the main components of micro-/nanohierarchical structures physically engineered on surfaces according to function and shape (**Table 1**), summarizing the recent research trends and potential applications while focusing on the combinations of different components with unique functionality (**Figure 1** and **Table 2**). Initially, we deal with the materials and methods used to fabricate each hierarchical structure type and discuss representative examples and their structural characteristics. Several recent strategies developed to overcome the existing limitations and realize better-performing hierarchical structures are presented, and their diverse niche applications (e.g., hydro-/omniphobic surfaces, bioinspired adhesives, electrodes/membranes for energy conversion/storage/harvesting devices, and physical/chemical/biological sensors) as well as basic working principles and requirements are discussed. Finally, we mention the existing challenges and present future research directions.

2. Types of Micro-/Nanohierarchical Structures Physically Engineered on Surfaces

As discussed in the Introduction section, the main components of hierarchical structures can be categorized into five types (rationally designed micropatterns, wrinkles, fibers (high-aspect-ratio pillars), ordered nanopatterns, and random structures) according to their main functions and shapes. Ordered-nanopattern-based hierarchical structure is excluded from this review because, with the exception of a few optical applications, ordered nanopatterns mainly act as secondary structures rather than primary structures. Usually, ordered nanopatterns are used as primary structures to facilitate a main function only in optical applications, such as nanophotonic devices based on plasmonic phenomena. However, these nanophotonic devices can be realized using only ordered nanopatterns without any supporting hierarchical structures and are, therefore, outside the scope of our review. In terms of performance enhancement, typically, ordered nanopatterns support the main function of the primary structure through synergistic effects. For instance, recent studies have demonstrated that ordered nanopatterns and wrinkle hierarchical structures can improve contact angle and TENG performance, but the effect is primarily due to wrinkles, and the ordered nanopatterns had a supporting synergistic effect.[62] Another example is contact angle manipulation using hierarchical structures based on ordered nanopatterns and micropyramidal arrangements. Previous research revealed that the micropyramid pattern functioned as the primary structural element for manipulating contact angle and mechanical properties, while the ordered nanopatterns had a supplementary role.[51] Nevertheless, ordered nanopatterns have been widely used as secondary structures in various hierarchical structures for improving hydrophobicity and modulating surface roughness.[63,64] Therefore, herein, we describe only four types of hierarchical structures, i.e., those with rationally designed micropatterns, wrinkles, fibers, and random structures as the primary component.

2.1. Physically Engineered Hierarchical Structures Based on Rationally Designed Micropatterns

When used as the primary component, rationally designed micropatterns can not only provide advantageous mechanical

© 2023 Wiley-VCH GmbH

15214095, 2024, 2, Downloaded from https://onlinelibrary.wiley.com/doi/10.1002/adma.202300871 by Korea Advanced Institute Of, Wiley Online Library on [14/01/2024]. See the Terms and Conditions (https://onlinelibrary.wiley.com/terms-and-conditions) on Wiley Online Library for rules of use; OA articles are governed by the applicable Creative Commons License

15214095, 2024, 2, Downloaded from https://onlinelibrary.wiley.com/doi/10.1002/adma.202300871 by Korea Advanced Institute Of, Wiley Online Library on [14/01/2024]. See the Terms and Conditions (https://onlinelibrary.wiley.com/terms-and-conditions) on Wiley Online Library for rules of use; OA articles are governed by the applicable Creative Commons License

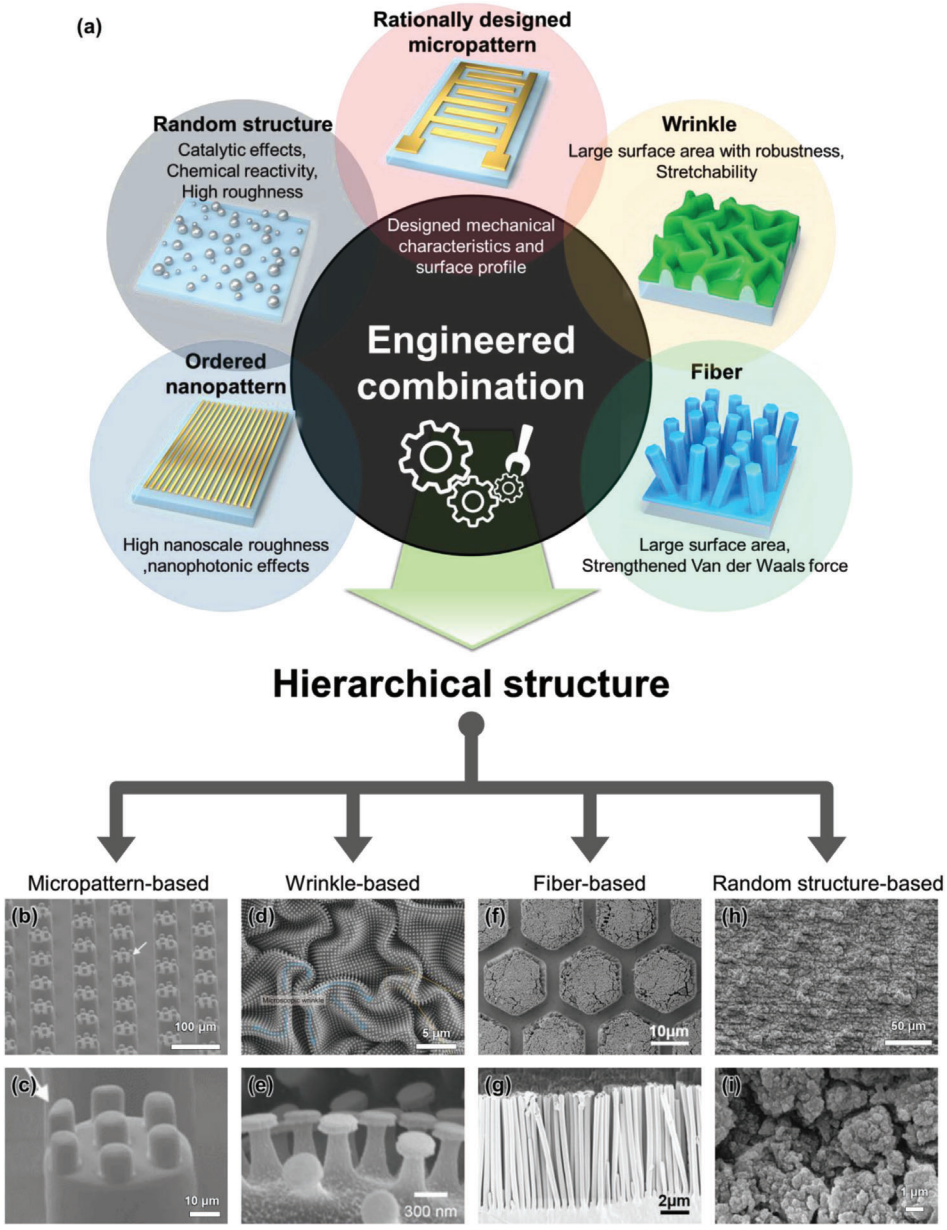


Figure 1. Hierarchical structures obtained by combining two different components. a) Schematic illustrations of the five components classified according to their main function and shape. b) Representative SEM image of micropattern-based hierarchical structure combining microscale tips and micropillars. c) High-magnification image of the structure in (b). b,c) Reproduced with permission.[7] Copyright 2009, Wiley-VCH. d) Representative SEM image of wrinkle-based hierarchical structure composed of T-shaped nanostructures on a wrinkled microstructure. e) Side-view image of the structure in (d). d,e) Reproduced with permission.[6] Copyright 2018, The Authors, Published by American Association for the Advancement of Science. From ref. [6]. © The Authors, some rights reserved; exclusive licensee AAAS. Distributed under a CC BY-NC 4.0 license http://creativecommons.org/licenses/by-nc/4.0/. Reprinted with permission from AAAS. f) Representative SEM image of fiber-based hierarchical structure featuring microscale patterned polystyrene nanopillars. g) Side-view image of the structure in (f). f,g) Reproduced with permission.[13] Copyright 2017, American Chemical Society. (https://pubs.acs.org/doi/10.1021/acsnano.7b04994; further permissions related to the material excerpted should be directed to the ACS) h) Representative SEM image of a random-structure-based hierarchical structure featuring microscale valleys and ridges. i) High-magnification image of the structure in (h). h,i) Reproduced under the terms of the CC-BY Creative Commons Attribution 4.0 International license (https://creativecommons.org/licenses/by/4.0) license.[60] Copyright 2020, The Authors, Published by MDPI.

properties such as high stability, strength, and flexibility, but also allow for the microscale construction of the designed surface profiles with high uniformity. In general, rationally designed micropatterns are fabricated using top-down processes including photolithography,[45–49] reactive ion etching, and e-beam evaporation[65] and can act as molds for elastomers (e.g., soft lithography).[66–68] Despite their high quality (i.e., precise patternability and process reproducibility), micropatterns fabricated by top-down processes have several drawbacks. For example, simple, planar single micropatterns are notvery functional

 © 2023 Wiley-VCH GmbH

Table 2. Representative examples (grouped according to unit components, unique characteristics, and applications) of recently reported micro-/nanohierarchical structures constructed by combining two or more components.

Reference	Primary structure	Secondary structure	Unique characteristics	Applications
	Fabrication method	Fabrication method		
[20]	Rationally designed micropattern (PDMS)	Rationally designed micropattern (PDMS)	Hierarchical structure with different shapes, mechanical properties tuned according to structure dimensions, inspired by gecko's toe pads to enhance van der Waals forces and contact splitting principle	Bioinspired dry/wet adhesives for industrial automated processes, robots, smart manipulators, grippers
	Photolithography and casting	Photolithography and casting		
[69]	Rationally designed micropattern (Metal)	Nanopattern (Metal)	Structure nanotransferred onto an arbitrary surface without chemicals, optical properties adjusted by rationally designed nanopattern to achieve enhanced security pattern	Raman spectroscopy (SERS) substrates, security patterns, optics, metamaterials
	Photolithography and e-beam evaporation	Photolithography, e-beam evaporation, thermal treatment, and nanowelding		
[73]	Rationally designed micropattern	Random nanostructure (polyimide, single-walled carbon nannotubes (SWCNTs), MOFs, metal oxide)	High specific surface area, high specific capacitance, excellent electrochemical performance, simplicity, easy customization, and broad application scope	Energy storage devices (microbatteries, micro-supercapacitors), electronics
	Laser patterning on substrate	Laser processing		
[62]	Wrinkle (Dragon Skin and Au)	Rationally designed micropattern (Dragon Skin)	Superhydrophobicity, large contact area, mechanical robustness, nanoscale sharp pattern edge for electron concentration, and uniform mechanical contact/separation	Superhydrophobic TENGs for cough detection
		Ordered nanopattern (Au)		
	Attachment of stiff skin layer on prestrained elastomer followed by release	Photolithography		
		Nanotransfer printing		
[52]	Wrinkle (PS and PVP)	Wrinkle (PS and PVP)	Large effective area, highly enhanced catalytic behavior, and superaerophobicity	Catalytic substrate for hydrogen evolution reaction
	Thermal shrinkage of substrate with sacrificial layer	Thermal shrinkage of substrate with sacrificial layer		
[30]	Wrinkle (PDMS)	Random nanostructure (AgNWs)	Electrically conductive network, large contact area, high roughness, mechanical robustness, and pressure-dependent effective contact area	Mechanical energy harvester and self-powered pressure sensor based on TENG for electronic skin
	Plasma treatment of prestrained elastomer followed by release	Drop casting and embedding		

(*Continued*)

© 2023 Wiley-VCH GmbH

15214095, 2024, 2, Downloaded from https://onlinelibrary.wiley.com/doi/10.1002/adma.202300871 by Korea Advanced Institute Of, Wiley Online Library on [14/01/2024]. See the Terms and Conditions (https://onlinelibrary.wiley.com/terms-and-conditions) on Wiley Online Library for rules of use; OA articles are governed by the applicable Creative Commons License

Table 2. (Continued).

Reference	Primary structure	Secondary structure	Unique characteristics	Applications
	Fabrication method	Fabrication method		
[10,102,111]	Fiber (PSS and PDMS)	Rationally designed micropattern	Contact area enhancement, increased chemical reaction region, good adhesion properties, and superhydrophobicity	Dry adhesive, functional surface
	Imprinting using AAO template	Photolithography and molding		
[15]	Fiber (CNTs)	Rationally designed micropattern	Contact area enhancement, increase in van der Waals forces, good adhesion properties, and superhydrophobicity	Dry adhesive, functional surface, self-cleaning surface
	Transfer of aligned CNTs	Photolithography and molding		
[13]	Fiber (PDMS and PS)	Rationally designed micropattern	Contact area enhancement, increase in chemical reaction region, good adhesion properties, and superhydrophobicity	Bioinspired dry adhesive, functional surface
	Imprinting using AAO template	Molding and mechanical shear		
[116]	Random structure (PDMS)	Ordered nanopattern (PDMS)	Hydrophobicity, large surface area, high roughness, mechanical robustness, and dome-like surface morphology	TENG for mechanical energy harvesting, water harvesting device capturing water from fog
	Thermal expansion of randomly distributed microspheres	Nanoimprinting lithography		
[125]	Random structure (PDMS)	Random structure (Ag MFs)	Electrically conductive network, different scale contact mechanisms: i) nanoscale pressure-induced contact and ii) microscale compression-induced deformation	Wide-range pressure sensor for electronic skin
	Molding using sandpaper	Drop casting and embedding		
[115]	Random structure (polymer nanofibers)	Random structure (AgNWs and graphene flakes)	Electrically conductive network, mechanical robustness, high roughness, pressure-dependent effective contact area, and bulk free volume	Highly sensitive pressure sensors for physiological signal monitoring and detection of spatial pressure distribution
	Electrospinning	Electrospraying		

without secondary structures (e.g., microtip on micropillar), fabricated by additional top-down processes to obtain synergistic effects. In addition, single micropatterns do not provide surface property modification (e.g., hydrophilicity/hydrophobicity) or optical property, as those properties are achieved using nanostructures, and exhibit a relatively low surface area to volume ratio without add-on structures. Finally, unlike the facile and scalable processes used to fabricate wrinkles or random structures, top-down processes use expensive materials and equipment. Despite these limitations, owing to the strong advantages of top-down processes (i.e., precise patternability, reproducibility, and uniformity), rationally designed micropatterns can be combined with different components (micropattern–micropattern,[8,9,12,14,17] micropattern–wrinkle,[62] micropattern–nanopattern,[69,70] and micropattern–random structure[71–73] combinations) to produce physically engineered hierarchical structures with superior characteristics. Micropattern-based hierarchical structures have potential applications in fields such as sensors,[74] dry/wet adhesives,[7–24] optical security patterns,[69,70] bioelectronics,[73,75] wearable devices,[72,75] and energy storage devices.[72] In the following paragraph, we summarize the strategies used to construct practically applicable micropattern-based hierarchical

© 2023 Wiley-VCH GmbH

15214095, 2024, 2, Downloaded from https://onlinelibrary.wiley.com/doi/10.1002/adma.202300871 by Korea Advanced Institute Of, Wiley Online Library on [14/01/2024]. See the Terms and Conditions (https://onlinelibrary.wiley.com/terms-and-conditions) on Wiley Online Library for rules of use; OA articles are governed by the applicable Creative Commons License

structures and overcome the limitations of single-micropattern structures.

Hierarchical structures consisting of two components with different shapes (e.g., micropattern–micropattern) feature tunable mechanical properties and designable surface profiles suitable for target applications and have primarily been developed by researchers working on bioinspired adhesives.[7–24] Micropillars topped by microtips are a representative example of micropattern–micropattern hierarchical structures, and this structure can provide improved functionality (e.g., enhanced adhesion) compared to single micropatterns. Ding and co-workers fabricated micropattern–micropattern hierarchical structures by replica molding (a physical engineering method) using photolithography and soft lithography (**Figure 2**a).[23] In this case, a top-down photolithographic process was sequentially applied to both sides of a silicon wafer to fabricate a master mold for the hierarchical structure with rationally designed micropatterns (micropillars topped by microtips). The top side of the spin-coated photoresist (PR) layer was irradiated with UV light through a photomask, and the back side of the PR layer was then irradiated with UV light in a relatively short period of time (Figure 2a(i)). Subsequently, the PR layer was developed to complete a mold for the microtip-on-micropillar array in Figure 2a(ii). Finally, a soft elastomeric material, polydimethylsiloxane (PDMS), was poured into the mold (Figure 2a(iii)), and the hierarchical structure of the microtip-on-micropillar array was then replicated by demolding (Figure 2a(iv)). By integrating these processes into a roll-to-roll continuous production system, Kwak and co-workers not only enhanced productivity but also demonstrated the feasibility of using a dry-adhesive-based robotic arm for glass transportation.[17] Hensel and co-workers (Figure 2b) and Xue and co-workers (Figure 2c) also fabricated hierarchical structures consisting of micropillars and microtips for use as dry adhesives.[8,9,14]

Jeong and co-workers proposed nanowelding process, which is a physical engineering method, for a variable-scale micropattern–nanopattern physically engineered hierarchical structure to modify the surface properties of the rationally designed micropatterns and achieve optical property modulation (Figure 2d).[69] First, Au micropillar structures were generated on a wafer after the deposition of a thin Cr adhesion layer via e-beam evaporation using a shadow mask and e-beam evaporation (Figure 2d(i),e). In addition, a polymeric stamp produced by nanoimprint lithography was used as a designated stamp for nanotransfer. In the second step, the target material was deposited on the nanopatterned polymeric stamp by e-beam evaporation (Figure 2d(ii)), and nanotransfer was then conducted by modulating process conditions such as temperature, pressure, and time (Figure 2d(iii, iv),f). In this research, Jeong and co-workers developed a strategy for the nanopatterning (e.g., nanotransfer) on a micropattern, overcoming the disadvantages of e-beam-lithography-based nanopatterning (high cost, complicated process, time-consuming nature, and non-reusability) through the use of a nanowelding technique that can be applied to any curved target surface and does not require the presence of a chemical adhesive between nanopattern and target surface. In view of nanoscale optical property modulation, the hierarchical micropattern–nanopattern structure can potentially be used in security identification, optics, and metamaterials.[69,70]

As another option for micropattern-based physically engineered hierarchical structures, the combination of random structures with rationally designed micropatterns can resolve the issue of low surface area to volume ratio of single micropatterns and endow excellent chemical reactivity, electrical conductivity, high specific surface area, and catalytic activity. In addition, the fabrication method for micropattern–random structures can lead to a facile and scalable approach without expensive materials and equipment, compared to the fabrication method for single-micropattern structures. Zhou and co-workers proposed patterning by laser processing using a physical engineering method known as laser-induced carbonization (LIC) to generate micropattern–random hierarchical structures for micro-supercapacitors using metal–organic frameworks (MOFs) (Figure 2g). LIC provides process efficiency, as it does not involve common fabrication processes such as mask preparation, photolithography, etching, e-beam, sputtering, and liftoff. Initially, a solution containing functional organic materials is deposited on a substrate through drop casting (Figure 2g(i)). Then, microscale interdigitated electrodes are produced by CO_2 laser patterning (Figure 2g(ii, iii)). In the final step, the fabricated electrodes are washed off to remove the coated solution and residues and thus afford a micropattern-random hierarchical structure (Figure 2g(iv),h). LIC has also been used by other research groups for the scalable fabrication of micropattern-random hierarchical structures as micro supercapacitors for high-performance energy storage (Figure 2i).[71–73,75–77] Advances in patterning using CO_2 laser processing to fabricate micropattern–random hierarchical structures presented potential applications in wearable bioelectronics for diverse physiological signal measurements, such as measurements of electrocardiogram (ECG) and biochemical parameters (e.g., glucose, calcium, and pH) of sweat.[75,77] CO_2 laser processing technique described above is not the only method used to fabricate hierarchical structures. Other laser sources, such as nanosecond fiber laser[78] and femtosecond laser,[79,80] have also been used to create diverse hierarchical structures for various applications, including antireflective applications,[79,80] anti-counterfeiting applications,[79] and energy and sensing devices.[78]

Add-on structures such as other micropatterns, wrinkles, nanopatterns, and random structures have been actively developed to impart superior functionality to micropatterns (i.e., synergistic effect) that act as basis for the desired mechanical properties. In particular, micropattern–micropattern hierarchical structures have been mainly studied for application as dry/wet adhesives.[7,8,10–24] Micropattern–nanopattern hierarchical structures were developed to exhibit surface modification (e.g., hydrophobicity and hydrophilicity) and optical properties.[69,70] In view of their high specific surface area and excellent catalytic activity, micropattern–random hierarchical structures easily produced using LIC have been used to fabricate superior supercapacitors for energy storage devices and wearable electronics.[71–73,75,77] By combining the advantages of micropattern structures (e.g., precise patternability and reproducibility) and the synergistic effects of add-on structures (e.g., micropatterns, wrinkles, nanopatterns, and random structures), one can produce hierarchical structures free from the drawbacks of single-micropattern structures.

© 2023 Wiley-VCH GmbH

15214095, 2024, 2, Downloaded from https://onlinelibrary.wiley.com/doi/10.1002/adma.202300871 by Korea Advanced Institute Of, Wiley Online Library on [14/01/2024]. See the Terms and Conditions (https://onlinelibrary.wiley.com/terms-and-conditions) on Wiley Online Library for rules of use; OA articles are governed by the applicable Creative Commons License

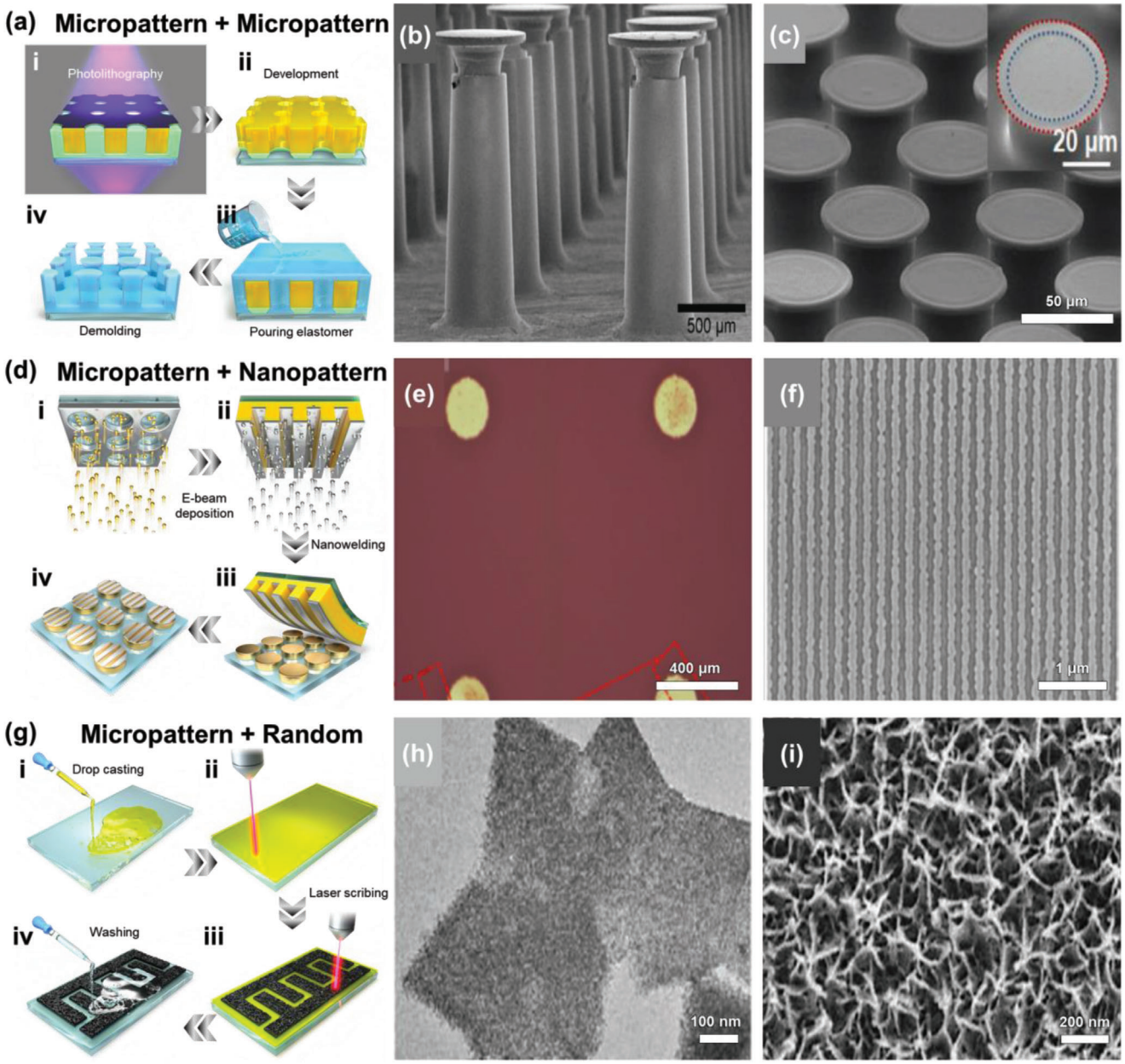


Figure 2. Various types of micropattern-based physically engineered hierarchical structures. a) Representative replica molding process used to fabricate hierarchical structures composed of two rationally designed micropatterns. b,c) SEM images present the structures in (a). b,c) Reproduced with permission,[9] Copyright 2019, The Authors, published by Wiley-VCH. c) Reproduced with permission,[14] Copyright 2020, Wiley-VCH. d) Representative nanowelding process used to fabricate hierarchical structures composed of rationally designed micropatterns and ordered nanopatterns. e,f) SEM images present the structures in (d). e,f) Reproduced with permission.[69] Copyright 2019, American Chemical Society. g) Representative patterning process by laser processing used to fabricate hierarchical structures composed of rationally designed micropatterns and random structures. h,i) SEM images present the structures in (g). h) Reproduced with permission,[70] Copyright 2021, Wiley-VCH. i) Reproduced with permission,[81] Copyright 2021, Elsevier.

2.2. Physically Engineered Hierarchical Structures Based on Wrinkles

When used as the primary component of hierarchical structures, wrinkles mainly provide highly dense multiscale curved structures with extremely large specific surface areas, mechanical robustness, and stretchability.[5,42,52,53,82–90] The fabrication of such structures has been inspired by the abundance of wrinkles in nature, as exemplified by plant surfaces[91] and fingerprints.[30] To mimic these designs, researchers have developed several methods of fabricating multilayered structures (e.g., stiff skin layers and soft substrates), as exemplified by the plasma treatment of elastomer substrates,[30] attachment of two different layers,[92] and use of a sacrificial skin layer.[52] Moreover,

© 2023 Wiley-VCH GmbH

15214095, 2024, 2, Downloaded from https://onlinelibrary.wiley.com/doi/10.1002/adma.202300871 by Korea Advanced Institute Of, Wiley Online Library on [14/01/2024]. See the Terms and Conditions (https://onlinelibrary.wiley.com/terms-and-conditions) on Wiley Online Library for rules of use; OA articles are governed by the applicable Creative Commons License

15214095, 2024, 2, Downloaded from https://onlinelibrary.wiley.com/doi/10.1002/adma.202300871 by Korea Advanced Institute Of, Wiley Online Library on [14/01/2024]. See the Terms and Conditions (https://onlinelibrary.wiley.com/terms-and-conditions) on Wiley Online Library for rules of use; OA articles are governed by the applicable Creative Commons License

several methods for generating strain on multilayer structures have been developed, including the application of prestrain to stretchable substrates (e.g., PDMS[93,94] and Dragon Skin[62]) before skin layer stacking and strain release as well as the heat treatment of thermally shrinkable substrates (e.g., polystyrene (PS)) with a skin layer.[83] Although these methods place limitations on the substrate material, i.e., require elastomeric or thermoplastic polymer substrates, they allow wrinkle structures to be relatively easily fabricated using large-area, facile, and low-cost processes and therefore hold great promise for both lab-scale and industrial applications. Based on the abovementioned merits, fabrication methods, and characteristics, numerous researchers have fabricated superior wrinkle-based hierarchical structures by combining wrinkles with other components (e.g., wrinkle–wrinkle,[52] wrinkle–micropattern,[43] and wrinkle–nanopattern[56]) and used these structures in applications such as strain sensors,[31,33] hydrophobic/hydrophilic surfaces,[85,95] and triboelectric energy harvesters.[62] However, some critical limitations (i.e., low design diversity and controllability, low material versatility, and low uniformity) due to the principle of wrinkle generation remain.[28,32,86,96–100] In the following paragraphs, we show how these limitations can be overcome and introduce recent strategies used to improve the synergistic effects of wrinkle-based hierarchical structures with different secondary components.

Hierarchical structures composed of multiple wrinkles with different feature sizes in a single substrate are widely used because of their large specific surface area, superior wettability, and stretchability. They are typically fabricated through the repeated formation of single-size wrinkles (**Figure 3**a). For example, Odom and co-workers developed a universal method for creating hierarchical wrinkles on thin-film surfaces.[52] As shown in Figure 3a, a sacrificial skin layer (e.g., polyvinylpyrrolidone (PVP)) is deposited on a thermally shrinkable substrate coated with the target material (e.g., gold, graphene, graphene oxide, WS_2, SnS_2, 1T-MoS_2, carbon nanotubes (CNTs), polyolefins, and polystyrene), with subsequent heating generating a strain mismatch between the sacrificial layer and the substrate. Then, the sacrificial layer is removed, and the first-layer wrinkles of the target material and the substrate are revealed. The authors controlled wrinkle wavelength by adjusting the thickness of the sacrificial layer at each step and showed that the developed method offers the benefit of material versatility and thus solves the bottleneck problem of wrinkle-based hierarchical structures (Figure 3b). In addition, these wrinkle–wrinkle hierarchical structures were shown to endow substrates with strain-independent functions.[5] As the valleys of the first-layer wrinkles absorb most of the strain energy, subsequent-layer wrinkles could maintain their features (including shape and function) even under an applied external strain of up to 100% (Figure 3c).

Alternatively, one can control wrinkle features and improve uniformity using rationally designed micropatterns. As discussed above, rationally designed micropatterns are frequently used to control the mechanical characteristics or surface profiles of substrates and can therefore also be applied to create elastic surface instabilities such as wrinkling, creasing, and deep folding in hierarchical structures. For example, Wang et al. reported a hierarchical structure composed of wrinkles and a periodic microscale hole array.[43] To fabricate this structure, the authors micropatterned an elastomer substrate using a lithographically patterned SU-8 mold and then attached the patterned elastomer to another elastomer substrate under an applied prestrain (Figure 3d). The strain was subsequently released to form various wrinkles with micropatterns on the substrate. Wrinkle morphology could be controlled by considering the surface strain distribution, which was determined by micropattern shape and periodicity (Figure 3e). Zhang et al. developed 3D microlens array/wrinkle structure/silver nanoparticle hierarchical structures inspired by rose petals as a substrate for surface-enhanced Raman scattering (SERS) spectroscopy[34] (Figure 3f), claiming that the ordered micropattern array with wrinkles and nanoparticles guarantees an even distribution of SERS hot spots and thus secures excellent uniformity and high sensitivity.

Ordered nanopatterns can also be integrated with wrinkles to enhance the surface wettability of wrinkle-based hierarchical structures. Although the conventional fabrication method of wrinkle–nanopattern hierarchical structures resembles that of wrinkle–micropattern ones except for the use of nanopatterned and not micropatterned molds[93] (Figure 3g), researchers have focused on more advanced fabrication techniques relying on the application of a rationally designed nanopattern to boost the synergistic effects. Yun et al. fabricated a springtail-inspired hierarchical structure composed of wrinkles and a serif-T nanopattern through a combination of nanoimprinting and secondary sputtering lithographic techniques[6] (Figure 3h). This structure showed superomniphobicity (i.e., high static repellency) and extreme pressure resistance against water, ethylene glycol, and ethanol owing to the combined effects of dense wrinkles and the designed nanopattern. Ahn et al. developed a morphology-controllable wrinkled micro-/nanohierarchical structure[62] by integrating micropatterns, nanopatterns, and wrinkles on a single substrate. Each structural element could be individually controlled, which offered unlimited design diversity (Figure 3i). The authors claim to have developed an optimized superhydrophobic hierarchical structure by controlling and changing the individual components, which are directly related to the droplet contact mode (e.g., Cassie–Baxter and Wenzel states).

Overall, researchers are actively trying to achieve material and structural versatility and utilize the synergistic effects of hierarchical structures composed of wrinkles and other components by developing advanced fabrication methods. Therefore, follow-up research should allow hierarchical structures to be effectively used in various fields, especially as components of hydrophobic/hydrophilic surfaces and energy-related devices owing to their superior specific surface area and mechanical stability.

2.3. Physically Engineered Hierarchical Structures Based on Fibers

Fiber structures (including pillar structures with high (>10:1) aspect ratios), another major component of hierarchical structures physically engineered on surfaces, have been used to increase the surface contact area, bonding forces such as van der Waals and adhesion forces (by increasing the effective contact area), and chemical reactivity.[101,102] A number of fiber-based

 © 2023 Wiley-VCH GmbH

15214095, 2024, 2, Downloaded from https://onlinelibrary.wiley.com/doi/10.1002/adma.202300871 by Korea Advanced Institute Of, Wiley Online Library on [14/01/2024]. See the Terms and Conditions (https://onlinelibrary.wiley.com/terms-and-conditions) on Wiley Online Library for rules of use; OA articles are governed by the applicable Creative Commons License

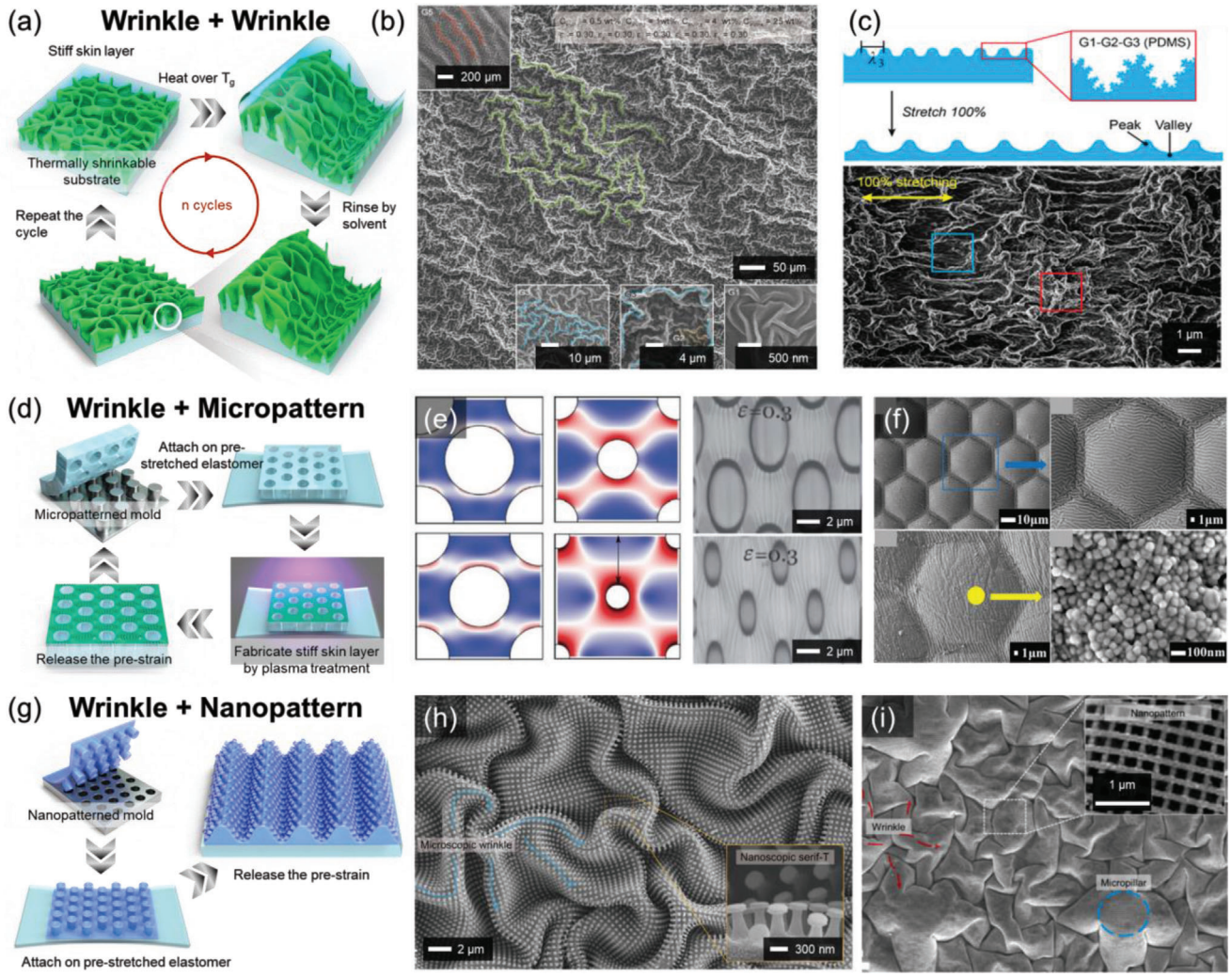


Figure 3. Various types of wrinkle-based hierarchical structures. a) Representative process used to fabricate hierarchical structures composed of multiple wrinkles and b) SEM images of the structures. b) Reproduced with permission.[52] Copyright 2018, American Chemical Society. c) Schematic illustration and SEM image of a hierarchical structure under an applied external strain of 100%. Reproduced with permission.[5] Copyright 2018, American Chemical Society. d) Representative process used to fabricate hierarchical structures composed of wrinkles and rationally designed micropatterns. e) Optical microscopy images of the structures. e) Reproduced with permission.[43] Copyright 2017, Wiley-VCH. f) SEM images of the structures. Reproduced with permission.[34] Copyright 2022, Wiley-VCH. g) Representative process used to fabricate hierarchical structures composed of wrinkles and ordered nanopatterns. h,i) SEM images of the structures. h) Reproduced with permission.[6] Copyright 2018, The Authors, Published by American Association for the Advancement of Science. i) Reproduced with permission.[62] Copyright 2021, Elsevier Ltd.

hierarchical structures are composed of nanofiber structures (primary structure) and rationally designed microstructures with patterns such as pillars, dots, and squares (secondary structure) fabricated using physical engineering methods. In view of the need for mechanical stability and strength to benefit from the advantages of the aforementioned fiber structure, rationally designed micropatterns are generally used as secondary structures. To take advantage of the fiber-based hierarchical structure, researchers have also attempted to imitate natural fiber structures (e.g., gecko's paws and tree frog's toes). To this end, various fabrication processes for fiber-based hierarchical structures have been developed, such as the formation of additional nanofiber structures using nanoscale molds on rationally designed micropatterns,[10] mechanical transfer of nanofibers (such as vertically aligned CNTs,[15] metal nanowires,[103] and polymer-based nanofibers[104]) on the microstructure, and combination of prefabricated nanofibers in micropatterns by post-treatment using mechanical shear forces.[13,21] Physical engineering methods of fabricating fiber-based hierarchical structures have limitations such as material selection (photocurable or thermoplastic polymers) due to the double molding requirement, the need for the high vertical alignment of transferred nanofibers to achieve structural uniformity, and the possibility of post-treatment-induced damage due to the mechanical weakness of nanofibers. Nevertheless, fiber-based hierarchies have been actively used because of their high surface area and suitability for contact area, chemical reaction region,

 © 2023 Wiley-VCH GmbH

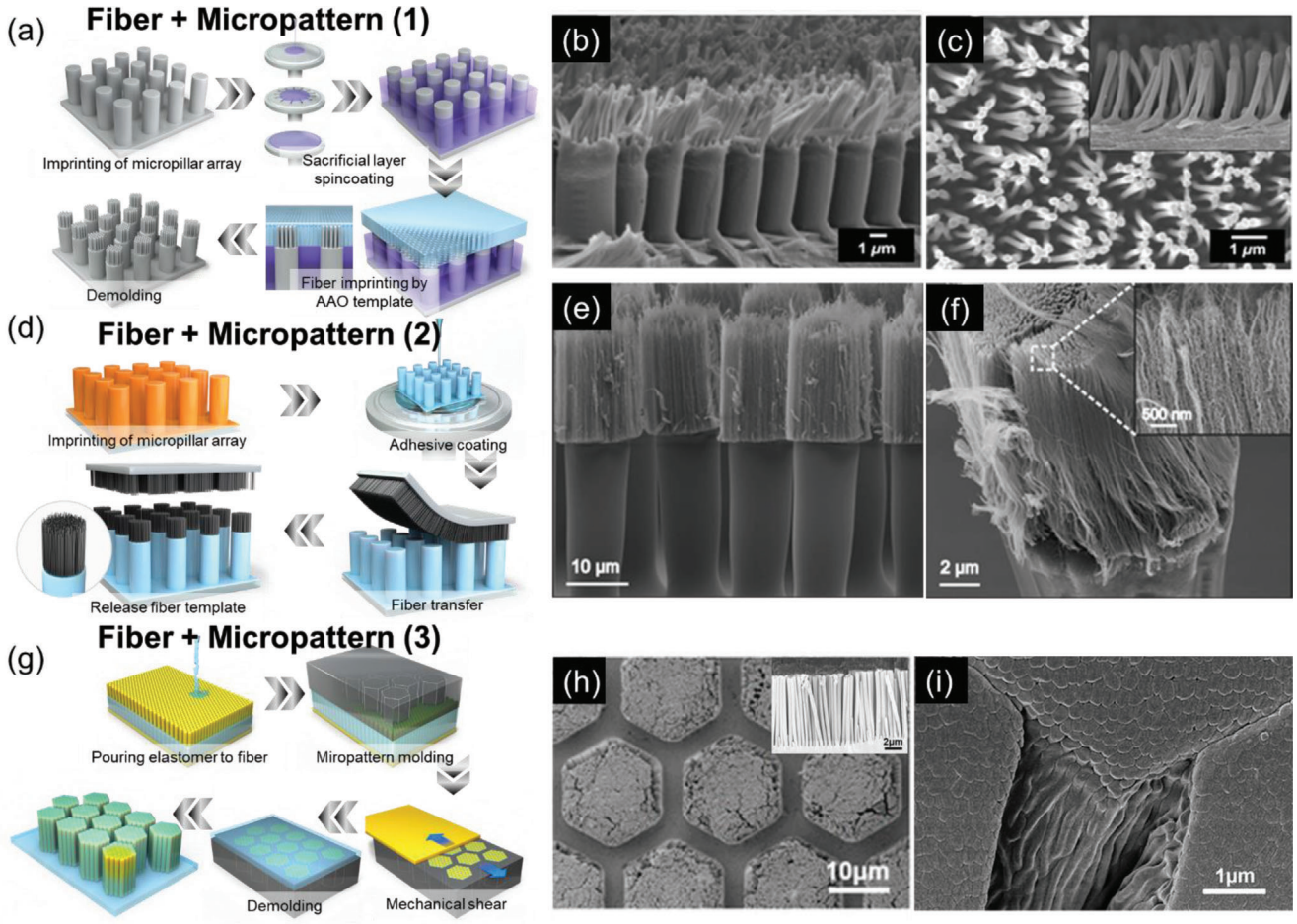


Figure 4. Various types of fiber-based hierarchical structures. a) Representative process used to fabricate nanoscale fiber-based hierarchical structures composed of high-aspect-ratio micropillars and nanofibers. b,c) SEM images of the structures in (a). b,c) Reproduced with permission.[10] Copyright 2018, American Chemical Society. d) Fabrication of heterogeneous-material-based hierarchical structures. e,f) SEM images of the structures in (d). e,f) Reproduced under the terms of the CC-BY Creative Commons Attribution 4.0 International license (https://creativecommons.org/licenses/by/4.0).[15] Copyright 2013, The Authors, published by Wiley-VCH. g) Representative process used to fabricate fiber-based hierarchical structures composed of embedded nanofibers in rationally designed micropillar structures using mechanical shear forces. h,i) SEM images of the structures in (g). g-l) Reproduced with permission.[13] Copyright 2017, American Chemical Society (https://pubs.acs.org/doi/10.1021/acsnano.7b04994; further permissions related to the material excerpted should be directed to the ACS).

and adhesion force enhancement. Nanofibers for fiber-based hierarchical structures can be fabricated using physical casting with anodic aluminum oxide (AAO) substrates,[10,105] while vertically aligned CNTs (or nanofibers)[106,107] are known to facilitate fabrication of fibers that could be modulated in length on demand. Furthermore, fiber-based hierarchical structures can be applied to the functional surfaces (e.g., hydrophilic and hydrophobic)[3] and dry adhesives[101] due to their modified surface properties and large reaction/contact area. Recent attempts to fabricate such structures as described above are introduced below.

This section introduces physical engineering methods for fiber-based hierarchical structures containing micro- or nanofibers for the abovementioned applications. As shown in **Figure 4**a, molds used to cast microfiber structures with high aspect ratios are generally manufactured using photolithography.[10,108] To this end, secondary micropillar structures composed of thermoplastic[109,110] and photocurable[111] materials have been fabricated using SU-8 and PDMS molds.[108] By contrast, nanoscale molds such as AAO templates are used to physically cast primary fiber structures based on poly(sodium4-styrenesulfonate) (PSS) via additional thermoforming or the precuring of photocurable materials. However, these casting methods can damage the micropillar structure shape during nanofiber formation due to oversoftening (or melting) of thermoplastics and uncurable regions of photocurable polymers. To overcome this limitation, the primary structures are protected by a sacrificial layer, and nanofibers are then molded on the top using an AAO template. Finally, the sacrificial layer is removed to afford a single-polymer-material fiber-based hierarchical structure. Figure 4b,c shows the production of a hierarchical structure consisting of fibers with uniform micro- and nanoscale dimensions and the fabrication of a substrate with a large-area hierarchical structure pattern.[111] The size and shape of base micropillars can be adjusted by changing the base mold fabricated by photolithography.[112] Furthermore, AAO templates can also

© 2023 Wiley-VCH GmbH

15214095, 2024, 2, Downloaded from https://onlinelibrary.wiley.com/doi/10.1002/adma.202300871 by Korea Advanced Institute Of, Wiley Online Library on [14/01/2024]. See the Terms and Conditions (https://onlinelibrary.wiley.com/terms-and-conditions) on Wiley Online Library for rules of use; OA articles are governed by the applicable Creative Commons License

control casting-mold porosity and size, enabling the molding of nanofibers with various and uniform diameters and lengths.[110] Thus, the size of the micro-/nanoscale hierarchical structure may be selectively adjusted.

In addition to hierarchical structures formed from a single material (by dual-curing process), a method of forming fiber-based hierarchical structures via selective mechanical transfer of heterogeneous materials to improve functionality (mechanical, chemical, and surface energy properties) has been developed. Figure 4d illustrates the formation of rigid SU-8-epoxy-based micropillars and the transfer of the vertically aligned CNT grown on the top onto the micropattern by physical contact.[15] For more stable nanofiber transfer, an adhesive material that improves the adhesion force should be applied on a surface. In general, the adhesive (e.g., poly(vinyl acetate)) is spin-coated on the micropillar structure array. Nanofibers can be easily and stably transferred by tilting the infrastructure shape or adjusting the diameter of contact area. Figure 4e,f shows the morphology of a heterogeneous fiber-based hierarchical structure consisting of SU-8 polymer-based microfibers at the bottom and highly aligned CNTs on top. Due to the improvement in adhesion by applying physical pressure and adhesive coating, a uniform and highly aligned fiber-transferred hierarchical structure could be fabricated. Furthermore, the hierarchical structure demonstrated improved mechanical stability and chemical stability due to the SU-8-based micropattern and the nanofibers such as CNTs, respectively. In addition, the hierarchical structure exhibited a broader application scope than a single-material hierarchical structure.

Finally, fiber-based hierarchical structures can be fabricated by physically binding nanofibers onto micropatterns. Figure 4g illustrates the manufacturing process of a nanofiber-based shape (thermoplastic polymer and photocurable polymer) using an AAO template–based mold.[13,105] The polymer was spin-coated on the manufactured nanofibers, and a bundle of nanofibers was then tied in micropattern units using a micropattern mold. The nanofibers contained in the mold were separated from the substrate using a mechanical shear force. When the support layer substrate was formed on the surface and separated from the mold, a hierarchical structure with nanofiber colonies distributed in micropattern units was formed (Figure 4h,i). The micropattern shape could be adjusted to produce nanofiber-based hierarchical structures with various micropatterns and improved mechanical performance.[15,111] Furthermore, this fabrication method allows the nanofiber tips to be embedded and directionally aligned. This process can embed nanofibers with micropatterns while minimizing nanofiber damage, thereby ensuring mechanical stability.

In summary, enhanced functionalities (e.g., adhesion force, chemical-reaction region, and reactive surface area) have been realized with uniform and stable fiber-based hierarchical structures, multiple material-based hierarchical structures, and nanofiber binding methods. These hierarchical structures have significant potential for use in a variety of applications, such as functional surfaces, dry/wet adhesives, and self-cleaning substrates. To modify surface and enhance the react/contact area for these applications, researchers have attempted uniform molding using AAO molds, transfer of mechanically strong and vertically aligned CNTs, and the embedding of nanofibers with elastomer polymers for the prevention of nanofibers' damage. These fiber-based hierarchical structures are expected to find applications in energy (e.g., solar cells with self-cleaning surfaces), biomedical (e.g., dry adhesives for surgery), and other industrial applications.

2.4. Physically Engineered Hierarchical Structures Based on Random Structures

Random structures (e.g., nanoparticles, nanowires, and microspheres) are frequently used as hierarchical structure components, as they can endow the surface with catalytic activity,[113] chemical reactivity,[114] and electrical conductivity[115] as well as increase specific surface area and roughness.[116] Over the past decades, many efficient fabrication methods for random structures have been reported, e.g., dry/wet etching,[117] chemical synthesis,[118] use of thermally expandable microspheres,[116] laser patterning,[119] and molding from naturally/artificially formed rough substrates.[117] Therefore, several uses of random structures as the main components of hierarchical structures resulted from superior versatility of the fabrication methods. In addition, researchers can select a compatible method easily according to the target materials and substrates for a wide range of applications that include supercapacitor electrodes,[118] physical/chemical sensors,[120–123] energy-harvesting devices,[116] and water-harvesting devices.[116] However, the use of random structures is generally associated with two main problems. The use of random structures can degrade sample-to-sample and in-sample uniformity, as these structures are literally random, unlike rationally designed micropatterns, ordered nanopatterns, and even wrinkles or fibers. Moreover, random structures suffer from low substrate adhesion, as most random nanomaterials are synthesized independently and then coated on the target substrates, while others (e.g., micropatterns or nanopatterns) are directly generated on the substrate surface. Although solving low uniformity issue of random structures is still challenging, there are a lot of advanced hierarchical structures for utilizing the abovementioned merits of the random structures. Thus, in the following paragraphs, we introduce recent strategies for overcoming these problems and discuss various types of random-structure-based hierarchical structures with unique characteristics and their applications.

The use of ordered nanostructures in combination with random microstructures may result in synergistic effects between large surface area and nanoscale roughness.[124] To fabricate nanopatterns on random microstructures, one should first form ordered nanopatterns and then use an additional process to add random structures, similarly to the case of wrinkle–nanopattern hierarchical structures (**Figure 5**a). Jung et al. reported a thermally expandable microsphere-based hierarchical structure with nanopatterns.[116] In this study, thermally expandable microspheres were mixed with a liquid elastomer precursor, and nanopatterns were generated on the cured elastomer through molding. The embedding of spin-coated microspheres inside the elastomer substrate secured mechanical robustness and macroscale uniformity. Subsequently, heat was applied to expand the embedded microspheres and thus fabricate a spherical hierarchical structure with nanopatterns on the surface. The effective surface area and roughness could be regulated via microsphere

© 2023 Wiley-VCH GmbH

15214095, 2024, 2, Downloaded from https://onlinelibrary.wiley.com/doi/10.1002/adma.202300871 by Korea Advanced Institute Of, Wiley Online Library on [14/01/2024]. See the Terms and Conditions (https://onlinelibrary.wiley.com/terms-and-conditions) on Wiley Online Library for rules of use; OA articles are governed by the applicable Creative Commons License

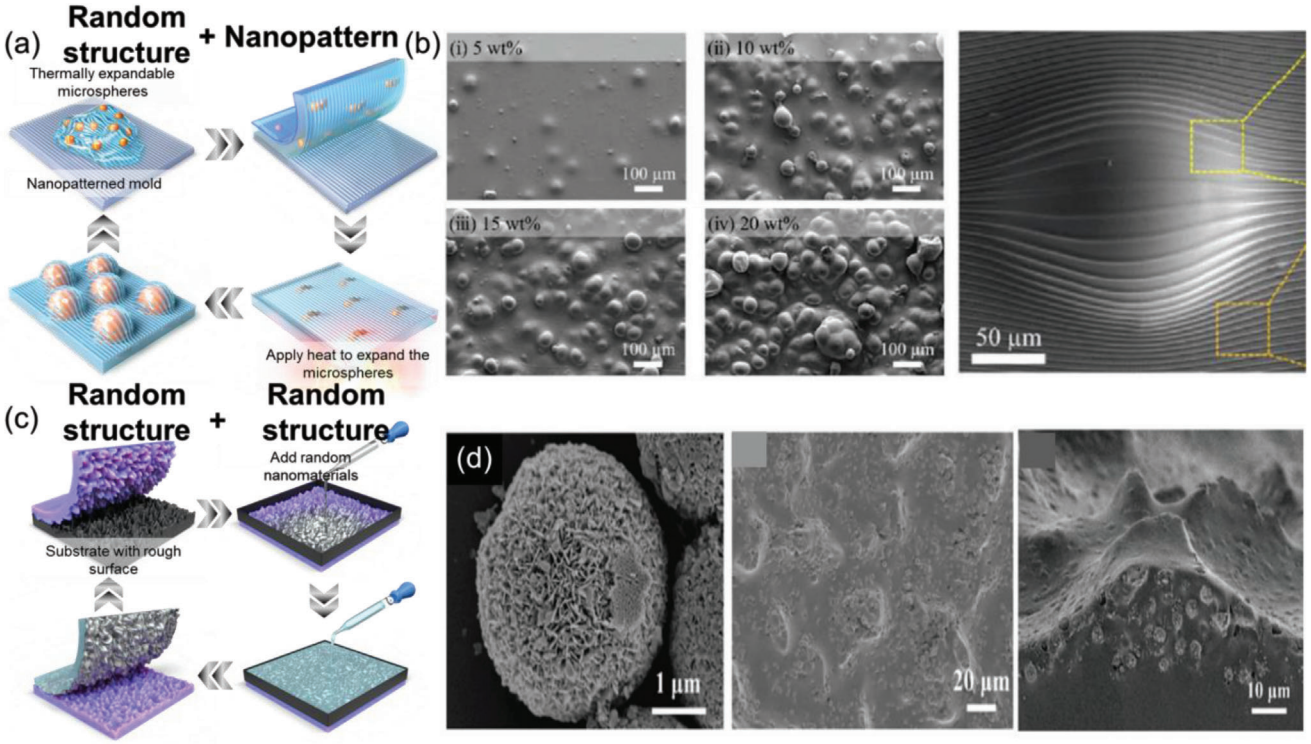


Figure 5. Various types of random-structure-based hierarchical structures. a) Representative process used to fabricate hierarchical structures comprising random structures and ordered nanopatterns. b) SEM images of the structures. c) Representative process used to fabricate hierarchical structures comprising multiple random structures by physical engineering of the surfaces. d) SEM images of the structures. b) Reproduced with permission.[116] Copyright 2022, Wiley-VCH. d) Reproduced with permission.[125] Copyright 2021, Royal Society of Chemistry.

density control (Figure 5b). These structures can be practically applied in water- and energy-harvesting devices because of their facile fabrication process and elevated surface area.

Random structure–random structure hierarchical structures are another type of random-structure-based hierarchical structures and are used to maximize fabrication efficiency and achieve multiscale surface roughness. To maximize these merits and secure mechanical robustness, researchers have adopted molding processes using artificially or naturally formed rough molds such as sand papers,[125] butterfly wings,[126] and lotus leaves[126] followed by the integration of randomly distributed nanomaterials such as graphene[115,120] and silver microflowers (Ag MFs[125]) (Figure 5c,d).[125] Generally, these structures were utilized as sensitive pressure sensors, as in the case of random microstructures, the contact area with the counterpart surface can drastically change with applied pressure, and the embedded nanomaterials impart electrical conductivity and allow sensitive contact area change at low pressures.[115]

Additionally, most random-structure-based hierarchical structures are fabricated using solution-based chemical synthesis.[127–129] These structures are widely used in applications requiring high-efficiency chemical reactions (e.g., battery anodes/cathodes,[127] supercapacitors,[130] catalysts,[113] chemical sensors,[114,121] and biosensors[131]) owing to their 3D reaction area. The related methods are more focused on chemical surface-engineering processes, such as hydrothermal synthesis and chemical bath deposition, rather than physical surface-engineering processes, such as molding and casting; as these methods are outside the scope of this review, they are not discussed in detail. However, several detailed reviews covering the fabrication, characteristics, and applications of the corresponding structures have been reported.[127,129,130,132] These reviews can shed light on the recent advances in random-structure-based hierarchical structures fabricated by chemical synthesis.

3. Applications

The unique physicochemical properties due to the synergistic effects of the abovementioned individual components have inspired researchers to utilize physically engineered hierarchical structures in various applications.[133–135] In this section, we categorize the major applications of the hierarchical structures into four groups, namely functional surfaces with controlled contact angles, dry/wet adhesives, energy-related devices, and physical/chemical/biological sensors. Each hierarchical structure is matched with proper applications in terms of its characteristics and application-imposed requirements, and the related limitations, recent advances, and perspectives are discussed.

3.1. Contact Angle Manipulation Using Designed Surface Profile for Functional Superhydrophobic/Superomniphobic Surfaces

The fabrication of functional surfaces based on hierarchical structures is made by the combination of the vari-

© 2023 Wiley-VCH GmbH

15214095, 2024, 2, Downloaded from https://onlinelibrary.wiley.com/doi/10.1002/adma.202300871 by Korea Advanced Institute Of, Wiley Online Library on [14/01/2024]. See the Terms and Conditions (https://onlinelibrary.wiley.com/terms-and-conditions) on Wiley Online Library for rules of use; OA articles are governed by the applicable Creative Commons License

ous (micro,[4,6,136–138] nano,[1–4,6,137,138] wrinkle,[5,6,51,62,88] and fiber[3,139,140]) structures introduced above. For functional surface fabrication, the structures used to design the Cassie–Baxter state mostly consist of rationally designed micropatterns and ordered nanopatterns (such as fibers, dots, and pillars). In particular, researchers have aimed to improve functionality through the application of hierarchical structures physically engineered on surfaces in the case of superhydrophobic[5,136–138,141] and superomniphobic[1,6,138] surfaces. The hierarchical structures of such functional surfaces are often inspired by nature, as exemplified by lotus leaves,[141–144] springtails,[1,6] Namibia beetles,[145,146] and mushrooms.[140,147,148] Most hierarchical structures contain substructures that follow the Cassie–Baxter state ($\cos\theta_{CB} = f_1\cos\theta_\gamma + f_2$, θ_{CB}: apparent contact angle, θ_γ: equilibrium contact angle, f_1: area fraction of solid, f_2: area fraction of air)[149] and therefore feature an air between patterns of these substructures. A microscale structural parameter study was reported to improve hydrophobicity by controlling the height, width, and distance between the structures.[150] The studies in the previous decades developed only superhydrophobic (water-repellent) surfaces[2,51,59,66,145,146] with contact angles of >150° and sliding angles of <10°. For example, Kim et al.[151] recently reported on a superhydrophobic surface with hierarchical structures fabricated by thermal imprinting and spraying. Integrating micropillars and random nanoparticles enabled superior superhydrophobicity with a contact angle of 163° and sliding angle of 7°. However, current studies focus on the development and application of superomniphobic surfaces[6,44] with high contact angles not only for water but also for oil, ethylene glycol, and ethanol.[3,4,138] **Figure 6**a shows a superomniphobic surface inspired by the hierarchical structure of the springtail.[6] Figure 6b shows a wrinkle–nanopattern shape in which a nanoscale disk is raised based on a microscale pillar whose width decreases with height. Such a structure is easy to use for producing superomniphobic surfaces, as the area of the air gap maintained at the interval between the pillars and the area in contact with the liquid are large. The contact angles of water, ethylene glycol, and ethanol changed upon the application of tension to the patterned wrinkled surface. When the surface was strained to 65%, the water contact angle remained almost unchanged at 158°, while the contact angles for ethylene glycol and ethanol changed from 140° to 150° and from 124° to 147°, respectively, because of the strain-induced changes in pattern arrangement (Figure 6c). This result shows how the hierarchical structure arrangement can be changed through the application of strain to the wrinkle structure.

Figure 6d shows a springtail-inspired hierarchical structure, with both the column and the disk prepared in nanoscale.[1] Dong et al. classified contact angle characteristics according to the spacing of the ordered nanohoodoo array. As shown in Figure 6e, the water contact angle exceeded 150° regardless of the pitch (290–1100 nm) and was the highest (156°) at a pitch of 800 nm. The contact angles for glycerol and ethylene glycol were also maximized at a pitch of 800 nm, which proved that omniphobicity can be increased using a high-aspect-ratio air gap. As described above, numerous attempts have been made to improve the contact angles of various liquids. The above surface can also be used to prevent fogging (Figure 6f).[3,152,153] In view of the excellent omniphobicity of this surface, fog droplets on the surface underwent agglomeration and could be removed via tilting by 20°. As a result, the omniphobic surface could be continuously maintained in a clean state.

Surface-modified micropattern–nanopattern-based hierarchical structures can be used in antifogging,[1,152,153] antifouling,[154–156] antimicrobial,[157,158] and self-cleaning[155,159,160] applications as well as for collecting spilled water–oil mixtures and oil leaked into the ocean (Figure 6g).[4] The surface did not exhibit a high contact angle against water, but was rather designed to be hydrophilic (water contact angle = 6°) and oleophobic (oil contact angle = 166°). Figure 6h shows the morphology of the functional surface presented in Figure 6g, revealing nanoscale cylinders and microscale pillars. With increasing nanocylinder's aspect ratio, the oil contact angle increased, while the water contact angle decreased (Figure 6i). In addition, Odom and co-workers developed stretchable superhydrophobic structures with a wrinkle-based hierarchy for use in flexible systems. As shown in Figure 6j, a PDMS-based wrinkle–random hierarchical structure exhibited superhydrophobicity and maintained a high-water contact angle (>150°) at a strain of 100%.[5] The water contact angle of the wrinkled surface was maintained at 160° during 1000 cycles (Figure 6k), and the corresponding contact angle hysteresis was below 3°. Therefore, the stretchable superhydrophobic surface was well suited for applications requiring twisting and bending (Figure 6l).

In summary, the current trend in hierarchical structures physically engineered on surfaces is the development and implementation of superhydrophobic and superomniphobic applications. In particular, bioinspired hierarchical functional surfaces are actively implemented, and industrial applications (e.g., antifogging, antifouling, antimicrobial, and self-cleaning) are being developed. Stretchable superhydrophobic surfaces hold great promise for the fabrication of flexible and bendable super-water-repellent systems, which can be used to achieve the self-cleaning and maintenance of marine sensor surfaces, self-cleaning solar cells, and water collection from alpine or desert areas.

3.2. Nature-Inspired Hierarchical Structures for Dry/Wet Adhesives

Given that micropatterns offer the advantages of precise patternability, reproducibility, uniformity, and tunable mechanical properties, micropattern–micropattern hierarchical structures with rationally designed surface profiles have been used for the fabrication of bioinspired adhesives. The high demand for dry/wet adhesives has been associated with fields such as medical devices,[18,21] industrial manufacturing,[20,161] robotic arms,[162,163] wearable electronics,[19,21] space,[164] and biomedical applications.[21,22,165] Many superior dry/wet adhesives have been inspired by nature, as exemplified by the adhesive pads of geckos,[7,10,14,16,20,25] octopus suction cups,[18,19,22,27] and the toe pads of tree frogs.[13,14,19,21] Such bioinspired dry/wet adhesives are mainly fabricated using hierarchical structures with different shapes (e.g., micropillars topped by microtips or micropillar arrays with cavities) to modulate the design parameters elaborately and mechanical properties of micropattern–micropattern structures (e.g., pillar diameter, height, gap distance of array, and cup diameter).

© 2023 Wiley-VCH GmbH

15214095, 2024, 2, Downloaded from https://onlinelibrary.wiley.com/doi/10.1002/adma.202300871 by Korea Advanced Institute Of, Wiley Online Library on [14/01/2024]. See the Terms and Conditions (https://onlinelibrary.wiley.com/terms-and-conditions) on Wiley Online Library for rules of use; OA articles are governed by the applicable Creative Commons License

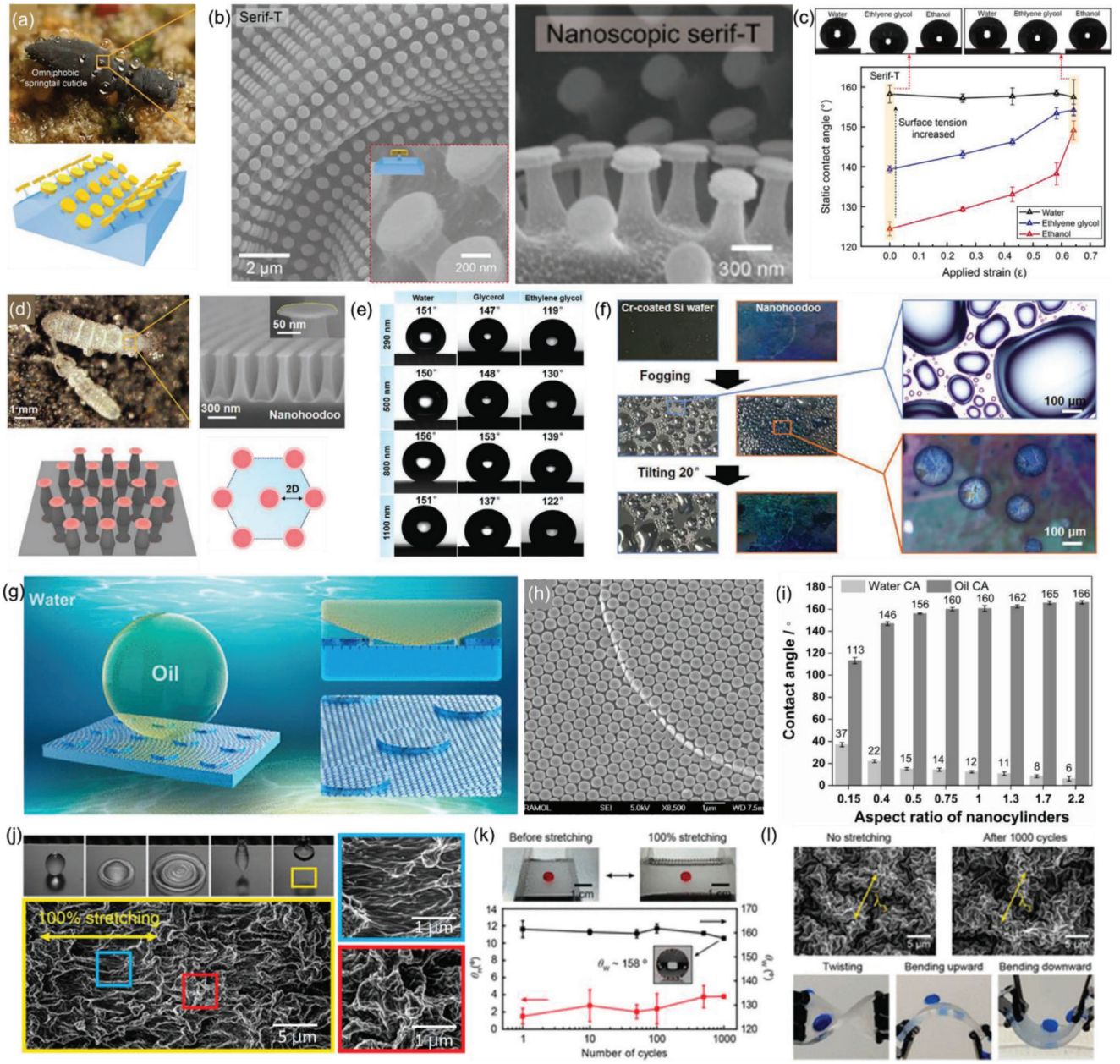


Figure 6. Applications of hierarchical structures as functional (e.g., superhydrophobic and superomniphobic) surfaces. a) Image of springtail and schematic structure of its superomniphobic surface. b) SEM image of wrinkled nanoscopic serif T-shape morphology. c) Contact angles for water, ethylene glycol, and ethanol under different strains. a–c) Reproduced with permission.[6] Copyright 2018, The Authors, Published by American Association for the Advancement of Science. d) Springtail-inspired nanohoodoo-based hierarchical structure used for superomniphobic surface construction and e) contact angles for water, glycerol, and ethylene glycol on the structure in (d). f) Antifogging application of the nanohood-based hierarchical structure (tilting angle = 20°). d–f) Reproduced with permission.[1] Copyright 2020, Wiley-VCH. g) Illustration of hydrophilic/oleophobic surface for collection of spilled water–oil mixtures. h) SEM image of the hierarchical structure in (g). i) Water and oil contact angle variation according to the nanocylinder's aspect ratio. g–i) Reproduced under the terms of the CC-BY Creative Commons Attribution 4.0 International license (https://creativecommons.org/licenses/by/4.0).[4] Copyright 2020, The Authors, published by American Chemical Society. j) Morphology of stretchable superhydrophobic surface. k) Results of water contact angle and hysteresis measurements at different strains. l) Twisting and bending tests of stretchable hierarchical structure and wrinkle morphology changes observed by SEM. j–l) Reproduced with permission.[5] Copyright 2016, American Chemical Society.

The numerous hierarchical structures (e.g., setae branching into terminal spatulae) in gecko's toe pads enable strong adhesion due to van der Waals interactions, as demonstrated by Full and co-workers.[166] Arzt et al. suggested that the adhesion force is related to not only the contact splitting principle (i.e., the adhesion force increases with the increasing number of hairs),[55] but also to two essential mechanical considerations of the hierarchical structure as follows. Two considerations are the stored elastic energy in the bulk of the hierarchical structure close to the contact surface and the interfacial stress created by the

© 2023 Wiley-VCH GmbH

15214095, 2024, 2, Downloaded from https://onlinelibrary.wiley.com/doi/10.1002/adma.202300871 by Korea Advanced Institute Of, Wiley Online Library on [14/01/2024]. See the Terms and Conditions (https://onlinelibrary.wiley.com/terms-and-conditions) on Wiley Online Library for rules of use; OA articles are governed by the applicable Creative Commons License

nonuniform contact between the hierarchical structure and the contact area.[61] Researchers have applied the concept of gecko's fibrillar toe pads in diverse emerging fields including manufacturing and robotics by mimicking biological structures using micropattern–micropattern hierarchical structures with different shapes (i.e., micropillars topped by microtips). Hu et al. developed a contact-sensible adhesive (CSA) inspired by a gecko's toe pad, which is composed of an adhesive layer based on a mushroom-shaped hierarchical structure and a capacitive sensing layer with a pair of foil electrodes (**Figure 7**a).[20] The side-view scanning electron microscopy (SEM) image of the CSA in Figure 7b shows the top adhesive layer and the bottom capacitive sensing layer. The pull-off force of CSA (7.8 N) was ≈3.7 times larger than that of the control sample (2.1 N) due to the hierarchical structure, which does not induce buckling, under the same preload of 8 N. For practical application, the CSA was integrated with a robotic gripper for grasping eggs with an additional weight and showed a change in capacitance ($\Delta C/C_0$) corresponding to the gripping action (Figure 7c).

Inspired by the dome-like protuberances of octopus suction cups, Pang and co-workers developed a micropattern–micropattern hierarchical structure for wet/dry adhesives using a molding process involving a solution-based air-trapping technique (Figure 7d).[22] The authors used the underlying mechanism of the octopus sucker, which attaches itself to the contact surface using an internal vacuum chamber formed by the temporary structural collapse of the sucker, to increase the adhesion force under water.[167] The related SEM image (Figure 7d) reveals a dense array of the octopus-inspired adhesive (OIA), which was replicated by filling a solution of a polyurethane-acrylate-based polymer into a master mold. Figure 7e presents confocal fluorescence microscopy images obtained while loading the OIA to demonstrate the liquid-assisted suction mechanism of OIA attachment under wet conditions. In this figure, stage I corresponds to the OIA in contact with a wet contact surface, and stage III shows the OIA with a lower vacuum chamber due to the capillary-driven suction of liquid toward the upper chamber. In addition, the OIA showed a higher conformal attachment (i.e., pull-off adhesion) pressure (≈25 kPa at a preload of 10 kPa) when attached to a wet contact surface than when attached to a dry contact surface and nonpatterned patch (≈5 kPa) (Figure 7f).

Tree frog's toe pads exhibit superior wet attachment and friction without preload, allowing them to easily climb up vertical flat surfaces (Figure 7g).[168] Jiang and co-workers developed a tree-frog-inspired adhesive (FIA), micropattern–micropattern hierarchical structure, that mimics the hierarchical structure of tree frog's toe pads and consists of a micro/nano two-level pillar array with nanocavities on the top of each pillar (Figure 7h).[21] By rationally designing FIA dimensions such as pillar size and channel width (Figure 7i), the authors effectively induced the self-splitting of liquids (i.e., the formation of nanometer-thick liquid films on the top of pillars) on the pillar array to generate a friction force ≈20-fold higher than that under dry or wet conditions. The FIA was further applied to a surgical tool to reduce damage to living tissue, which is a common problem of existing sharp-tooth surgical graspers requiring high external forces to grasp the tissue (Figure 7j). Compared to a conventional sharp-tooth surgical grasper, the FIA-based one showed an approximately fivefold higher normal force and a ninefold higher friction force while reducing the tissue deformation by 90%.

For superior properties of adhesive, Pang and co-workers developed a heterogeneous adhesive, micropattern–micropattern hierarchical structure, inspired by tree frog's toe pads and the convex cup of octopus suckers (Figure 7k).[19] The related SEM images (Figure 7l) revealed the presence of tree-frog-inspired hexagonal microchannels (upper) and octopus-inspired convex structures (lower). The hexagonal microchannels provided omnidirectional peel resistance and drainage to wet and rough surfaces, while the convex structures provided strong adhesion under various dry and wet conditions. Due to its hierarchical structure, the heterogeneous adhesive had a higher adhesion strength of 4.5 N cm^{-2} in underwater conditions compared to the flat adhesive with an adhesion strength of ≈0.5 N cm^{-2}. Figure 7m compares the results of the flow resistance test of the heterogeneous adhesive with those obtained for a flat PDMS patch in flowing water ($Q \approx 150$ mL cm^{-2} s^{-1}). In addition, the authors applied the heterogeneous adhesive to a wearable electronic device to detect ECG signals using a conductive material (Figure 7n).

To summarize, diverse adhesives for use under dry or wet conditions in fields such as biomedical engineering, industrial production, wearable electronic devices, and space have been developed because of their high demands. In particular, natural hierarchical structures (e.g., toe pads of geckos and octopus suction cups as well as tree frogs) provide hints or solutions for the development of superior bioinspired micropattern–micropattern hierarchical structures with different shapes that can be used as adhesives under diverse (dry, wet, and underwater) conditions. In the future, efforts to mimic the hierarchical structures in nature will be meaningful in various fields as state of the art of manufacturing technologies and biomimetic research progress.

3.3. Hierarchical Structures with Extremely Large Surface Area for High-Performance Energy Harvesting/Storage Devices

Micro-/nanohierarchical structures hold great promise for energy-related applications such as energy harvesting (e.g., TENGs),[58,62,169–177] storage (e.g., battery electrodes),[127,130,178] and conversion (e.g., electrolyte membranes of fuel cells)[28,179,180] as well as self-powered devices,[62,181] as the performance of most corresponding systems is directly related to the effective surface area, i.e., physical or chemical contact area. Given that most hierarchical structures physically engineered on surfaces provide high mechanical robustness compared with the chemically synthesized hierarchical structures as well as large specific surface area and roughness, they well meet the key requirements of high-performance TENGs,[62] which harvest electrical energy from wasted mechanical energy by exploiting the triboelectric effect (**Figure 8**a). In a TENG, an increase in specific surface area results in elevated electrified and contact areas, while an increase in nanoscale roughness increases the extent of electrification per unit area by inducing friction and electron concentration; moreover, mechanical robustness is required during the repeated physical contact between the electrified surfaces.[182] Thus, wrinkle-based hierarchical structures are preferred for TENG applications. Kang et al. reported a high-performance TENG based on Ag-nanowire (AgNW)-embedded

© 2023 Wiley-VCH GmbH

15214095, 2024, 2, Downloaded from https://onlinelibrary.wiley.com/doi/10.1002/adma.202300871 by Korea Advanced Institute Of, Wiley Online Library on [14/01/2024]. See the Terms and Conditions (https://onlinelibrary.wiley.com/terms-and-conditions) on Wiley Online Library for rules of use; OA articles are governed by the applicable Creative Commons License

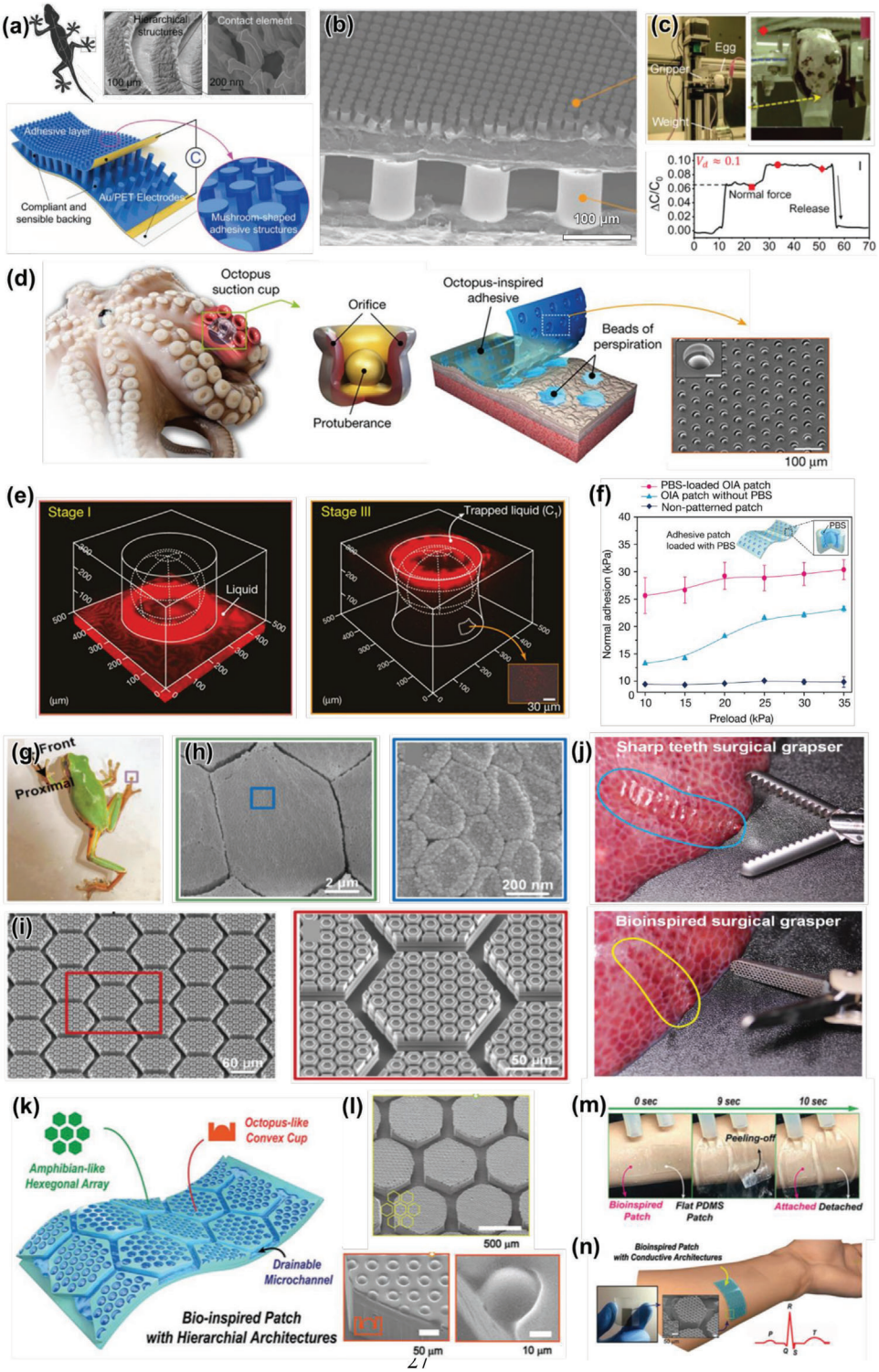


Figure 7. Hierarchical structures for dry/wet adhesive applications. a) Schematic illustration of gecko-inspired hierarchical structure for contact-sensible adhesive (CSA) application. b) SEM images of CSA composed of adhesion and sensing layers. c) Application of CSA in a mechanical gripper grasping an egg with an additional 300 g weight. Relative change in capacitance ($\Delta C/C_0$) corresponding to gripping motion. a–c) Reproduced with permission.[20] Copyright 2021, Wiley-VCH. d) Schematic illustration of octopus-suction-cup-mimicking hierarchical structure for wet/dry adhesives and related SEM image showing a dense array of these structures. e) Confocal fluorescence microscopy images used to verify the mechanisms of adhesive attachment under wet conditions. f) Pull-off adhesion as a function of preload. d–f) Reproduced with permission,[22] Copyright 2017, Macmillan Publishers Limited, part of Springer Nature. g) Photograph of tree frog climbing on a wet smooth surface. h) SEM images of tree frog's toe pad composed of micropillar epithelial cells (green) showing dense nanopillars with nanocavities in each micropillar (blue). i) SEM images of frog-inspired adhesive (FIA) showing

© 2023 Wiley-VCH GmbH

15214095, 2024, 2, Downloaded from https://onlinelibrary.wiley.com/doi/10.1002/adma.202300871 by Korea Advanced Institute Of, Wiley Online Library on [14/01/2024]. See the Terms and Conditions (https://onlinelibrary.wiley.com/terms-and-conditions) on Wiley Online Library for rules of use; OA articles are governed by the applicable Creative Commons License

15214095, 2024, 2, Downloaded from https://onlinelibrary.wiley.com/doi/10.1002/adma.202300871 by Korea Advanced Institute Of, Wiley Online Library on [14/01/2024]. See the Terms and Conditions (https://onlinelibrary.wiley.com/terms-and-conditions) on Wiley Online Library for rules of use; OA articles are governed by the applicable Creative Commons License

wrinkled PDMS produced by plasma treatment (Figure 8b).[30] The output voltage increased with the increment of plasma treatment power because of the concomitant wrinkle pattern enlargement and surface roughness enhancement (Figure 8c), while the embedded AgNWs provided an electrically conductive network for electron transfer. In addition, other components of hierarchical structures can be utilized for TENG construction to impart unique functions. Ahn et al. designed a wrinkle–micropattern–nanopattern hierarchical structure (Figure 8d)[62] to enhance TENG performance and to achieve water resistance (Figure 8e). Specifically, the output voltage increased from 13.6 to 16.5 V as the flat film was replaced by a nanopatterned film, and when wrinkles were added to nanopatterns, the voltage output of the TENG increased to a maximum of 35.9 V. Furthermore, when micropillars were added, the TENG voltage output was maximized to 48.0 V, exceeding that of the flat TENG by 608%. Wrinkles and nanopatterns provided a large surface area and mechanical robustness. Micropatterns facilitated uniform contact and separation for the formation of a large dipole moment between electrodes. Additionally, nanopatterns imparted superhydrophobicity and allowed the TENG to rapidly recover from water droplets (Figure 8f).

In view of their large multiscale surface area and wide-range material applicability, hierarchical structures physically engineered on surfaces can also be used for energy storage/conversion. Lee et al. used a wrinkle–wrinkle hierarchical structure in the architecture of the interface between a polymer electrolyte membrane and the catalyst layer of a fuel cell (Figure 8g).[28] The multiscale (nano- to micrometer) hierarchical wrinkles allowed one to go beyond the limit of catalyst utilization, and the resulting multiscale wrinkle interface therefore showed a dramatically increased (by up to 89% compared to flat-interface values) electrochemically active surface area and power performance. Cho et al. developed a micropattern–nanopattern hierarchical structure through a LEGO-like integration of multiscale patterns (Figure 8h)[179] and used it to fabricate a Nafion-membrane fuel cell with significantly enhanced electrochemical performance and sufficient mechanical robustness. Random-structure-based hierarchical structures are preferred for such applications, as they offer the benefits of superior catalytic effects and 3D reaction area, while other structures can react only at the top surface area. As discussed in Section 2.4, most random-structure-based hierarchical structures are fabricated using solution-based chemical synthesis and are therefore outside the scope of this review. For further details on random-structure-based hierarchical structures used in energy-related applications such as Li-ion batteries, supercapacitors, and fuel cells, the readers should consult specialized reviews.[127,130,132,178]

In summary, hierarchical structures physically engineered on surfaces have significant potential for use in energy-related applications. Wrinkle-based hierarchical structures are mainly used in TENGs because of their mechanical robustness, while random-structure-based hierarchical structures are used in battery electrodes and electrolyte membranes owing to their large surface area and facile fabrication methods. However, despite the efforts made to improve device performance, cost-effective and mass-production-suitable fabrication methods should be further developed to commercialize hierarchical-structure-based energy-related devices, as cost-effectiveness and producibility are the main factors of influence in these fields. We believe that state-of-the-art studies should facilitate the development of facile manufacturing methods and that follow-up research will allow hierarchical structures to be practically commercialized.

3.4. Hierarchical Structures with Extremely Large Surface Area for Highly Sensitive Physical/Chemical/Biological Sensors

Hierarchical structures physically engineered on surfaces, including micro-/nanoscale components, have been actively researched for application in sensors, which can be classified into physical sensors,[31–35,37,74] chemical sensors,[36,183–186] and biological sensors.[34,131,187,188] Among various reasons for applying hierarchical structures in sensors, the most important one is to improve the sensitivity and sensing speed. Many hierarchical-structure-based sensors contain rationally designed micropatterns as the primary substrate (or framework) because of their superior mechanical stability, and wrinkle or random structures as the secondary structure because of their elevated reactive surface area. In this section, we introduce the morphological properties of hierarchical structures and their use in physical, chemical, and biological sensors. Initially, hierarchical-structure-based physical sensors for pressure and strain were developed to increase the sensitivity and sensing range.[31–33,35,37,74,189] In particular, the implementation of micro-/nanohierarchical structures (e.g., microdomes–wrinkle,[189] V-groove–wrinkle,[31] and multiscale wrinkle[190]) aims to enhance the performance of physical sensors by increasing the extent of physical deformation and contact area variation in response to external forces and tensions. In the case of pressure sensors, a PDMS-based capacitive pressure sensor with micropattern–nanopattern (micropapillae and nanoscale folds) mimicking rose petals was developed (**Figure 9**a).[35] This sensor consists of a single and double layer of a well-defined PDMS structure with indium tin oxide electrodes and can sensitively detect both static and dynamic pressures. Figure 9b describes the performance of this biomimetic pressure sensor. The ultrasensitive capacitive pressure sensor showed a sensitivity of 0.055 kPa^{-1} and could detect a wide range of pressures (0.5–10 kPa) in 200 ms. Very thin (≈32 μm) micro- and nanostructures have been demonstrated to dramatically improve the pressure sensitivity, especially at low pressures (1–5 kPa). In the case of strain sensors, hierarchical structures were

concave pillar surface with two-level pillars and channels. j) Medical application of FIA in surgical grasper. g–i) Reproduced under the terms of the CC-BY Creative Commons Attribution 4.0 International license (https://creativecommons.org/licenses/by/4.0).[21] Copyright 2020, The Authors, published by Wiley-VCH GmbH. k) Schematic illustration of heterogeneous adhesive inspired by tree frog's toe pads and the convex cup of an octopus sucker. l) SEM images showing tree-frog-inspired hexagonal microchannels and octopus-inspired convex structures. m) Flow resistance test of heterogeneous adhesive in flowing water. n) Schematic illustration of ECG signal detection using heterogeneous adhesive with conductive materials. k–n) Reproduced with permission.[19] Copyright 2019, Wiley-VCH.

 © 2023 Wiley-VCH GmbH

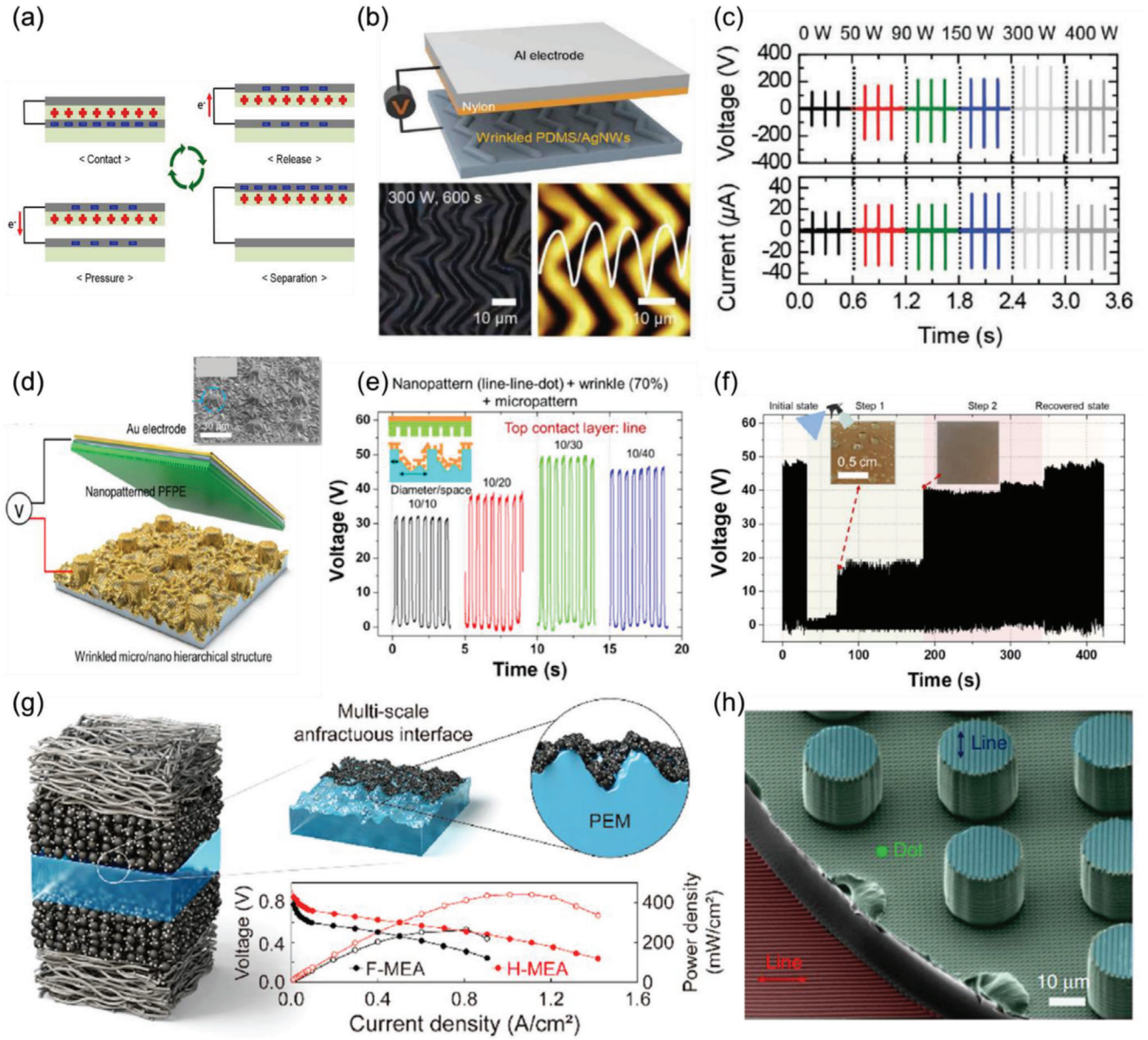


Figure 8. Micro-/nanohierarchical structures used in energy-related applications such as TENGs and fuel cells. a) Schematic working principle of TENGs. Reproduced with permission.[182] Copyright 2022, Wiley-VCH. b) Schematic illustration and optical microscopic images of TENG using wrinkle-based hierarchical structure. c) Triboelectric performance of such TENGs with oxygen-plasma-treatment-power-controlled wrinkle sizes and densities. b,c) Reproduced with permission.[30] Copyright 2019, Wiley-VCH. d) Schematic illustration and SEM image of superhydrophobic TENG featuring wrinkle-based hierarchical structure. Reproduced with permission.[62] Copyright 2021, Elsevier. e) Triboelectric performance achieved for different rationally designed micropatterns. Reproduced with permission.[62] Copyright 2021, Elsevier. f) Triboelectric performance achieved upon water spraying. Reproduced with permission.[62] Copyright 2021, Elsevier. g) Schematic illustration of catalyst layer/membrane interface using wrinkle-based hierarchical structure for ultralow Pt-loading polymer electrolyte membrane fuel cells. Reproduced with permission.[28] Copyright 2022, American Chemical Society. h) Colored SEM image of Lego-like rationally designed micropattern-based hierarchical structure used in polymer electrolyte membrane fuel cells. Reproduced under the terms of the CC-BY Creative Commons Attribution 4.0 International license (https://creativecommons.org/licenses/by/4.0).[179] Copyright 2015, The Authors, published by Springer Nature.

fabricated using nanomaterials such as metal nanowires,[33] metal nanoparticles,[31] and MXenes[37] for nanoscale random structures. Figure 9c shows a MXene/polyaniline-fiber (PANIF)-based tile-like stacked hierarchical structured composite[36,37,183,185] consisting of microscale MXene wrinkles produced using a prestrained rubber substrate and nanoscale PANIF. Figure 9d shows the performance of this hierarchical strain sensor, revealing a broad sensing range (up to 80% strain), high sensitivity (gauge factors of up to 2369.1), an ultralow detection limit (0.1538%), possibility of wireless biomonitoring, and excellent stability under cyclic strain. Figure 9e presents the results of strain detection in

© 2023 Wiley-VCH GmbH

15214095, 2024, 2, Downloaded from https://onlinelibrary.wiley.com/doi/10.1002/adma.202300871 by Korea Advanced Institute Of, Wiley Online Library on [14/01/2024]. See the Terms and Conditions (https://onlinelibrary.wiley.com/terms-and-conditions) on Wiley Online Library for rules of use; OA articles are governed by the applicable Creative Commons License

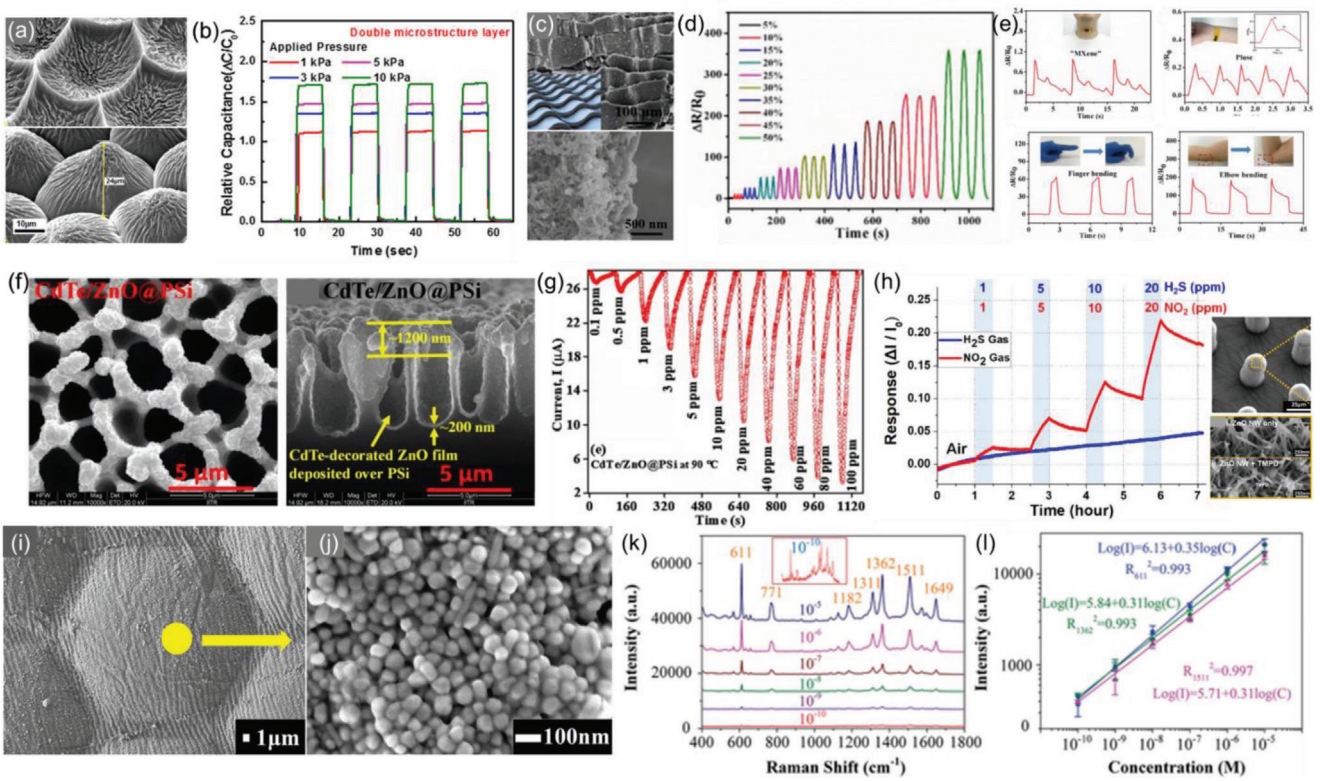


Figure 9. Applications of hierarchical structures in physical, chemical, and biological sensors. a) Morphology of capacitive pressure sensor with a red-rose-petal-mimicking hierarchical structure. b) Pressure sensor performance and sensing range (0.5–10 kPa, response time below 200 ms). a,b) Reproduced with permission.[35] Copyright 2020, Elsevier. c) Wrinkle/nanofiber hierarchical structure of MXene-based nanocomposite strain sensor. d) Strain sensing performance at strains of 0–50%. e) Detection of human body strain by developed strain sensor. c–e) Reproduced with permission.[37] Copyright 2020, Elsevier. f) Morphology of random hierarchical structure of CdTe–ZnO for NO_2 gas sensor. g) Results of NO_2 gas sensing (0.1–1000 ppm). f,g) Reproduced with permission.[36] Copyright 2021, Elsevier. h) NO_2 gas sensing performance (1, 5, 10, and 20 ppm) of TMPD-coated micropost–ZnO-nanowire-based hierarchical gas sensor. Reproduced with permission.[121] Copyright 2020, American Chemical Society. i,j) Morphology of hierarchical biosensor used to detect water pollution. The structure consists of microscale honeycombs and nanoscale wrinkles (mimicking rose petals). Ag nanoparticles were grown on the top surface for SERS application. k,l) SERS results obtained for rhodamine 6G (k) and various water samples (deionized water, lake water, tap water, spring water, and river water) (l). i–l) Reproduced with permission.[34] Copyright 2021, Wiley-VCH.

various parts of the human body (voice, wrist, finger, and elbow).

Furthermore, chemical sensors (e.g., gas sensors) using random-structure-based hierarchical structures have been developed.[36,183,185] In the field of chemical sensing, much attention has been drawn to increasing the reactive surface for improving sensitivity and sensing speed. Therefore, many researchers have tried to apply nanoscale hierarchies to provide larger reaction surface to the sensing elements. The random morphology of fabricated hierarchical CdTe-functionalized ZnO (CdTe–ZnO) gas sensor on a porous Si substrate is shown in Figure 9f.[36] It showed superior sensitivity and rapid sensing capability because of its high reactive surface area (Figure 9g), detecting NO_2 gas at levels of 0.3–100 ppm and fast response/recovery times of ≈13/54 s at 90 °C. Micropost pattern and ZnO-nanowire-based gas sensor with *N,N,N′,N′*-tetramethyl-*p*-phenylenediamine (TMPD) coating, physically cast via an SU-8 mold, was analyzed for its NO_2 gas sensing capabilities (Figure 9h). The sensing mechanism relied on the color change arising from the interaction between the TMPD and NO_2 gas. Additionally, the high aspect ratio micropost contributed to a larger surface area, leading to an improved sensing performance of the NO_2 gas sensor. As a result, the detection of NO_2 gas at fine concentrations such as 1, 5, 10, and 20 ppm has been reported.[121]

Finally, hierarchical structures have also been applied to biological sensors, which are widely used for applications in the healthcare, disease diagnosis, and environmental protection. Lutao and co-workers developed a biosensor based on micropattern–nanopattern (such as rose-petal-inspired micro-nanopattern) hierarchical structure for environmental protection and drug detection.[34] Figure 9i,j shows the morphological characteristics of the sensor hardware consisting of a microlens structure and nanoscale wrinkles. Ag nanoparticles were grown for the application in SERS spectroscopy, and the nanogaps between these nanoparticles enhanced the analytical performance by generating plasmonic hotspots. Notably, the ordered micro-nanohierarchical structure array could expand the multidimensional distribution of hotspots to achieve superior sensitivity and could also ensure an even hotspot distribution to obtain superior uniformity. Figure 9k presents the SERS spectra of rhodamine 6G at different concentrations. The hierarchical-structure-based

© 2023 Wiley-VCH GmbH

15214095, 2024, 2, Downloaded from https://onlinelibrary.wiley.com/doi/10.1002/adma.202300871 by Korea Advanced Institute Of, Wiley Online Library on [14/01/2024]. See the Terms and Conditions (https://onlinelibrary.wiley.com/terms-and-conditions) on Wiley Online Library for rules of use; OA articles are governed by the applicable Creative Commons License

15214095, 2024, 2, Downloaded from https://onlinelibrary.wiley.com/doi/10.1002/adma.202300871 by Korea Advanced Institute Of, Wiley Online Library on [14/01/2024]. See the Terms and Conditions (https://onlinelibrary.wiley.com/terms-and-conditions) on Wiley Online Library for rules of use; OA articles are governed by the applicable Creative Commons License

3D-SERS substrate showed the highest Raman signal enhancement. Figure 9l presents the SERS spectra of Malachite green (10^{-6} M) in river water, spring water, tap water, lake water, and deionized water (from bottom to top) recorded to verify the ability of the sensor to detect water pollution.

In summary, research on the sensitivity, sensing speed, and performance improvement through the use of hierarchical structures physically engineered on surfaces is ongoing. The improvement of the surface area of the sensor plays a major role in increasing the sensitivity and contributes to the improvement of sensing performance and detection range. To this end, researchers have attempted to form various hierarchical structures by mimicking plants (e.g., rose petals) or growing metal oxide or metal nanostructures. As a result, the sensitivity and performance of physical, chemical, and biological sensors have been enhanced, and sensors for wearable, healthcare, and environmental protection applications have been developed. Furthermore, current research aims to address the challenges of large area, mass production, and uniformity improvement to realize the commercialization of hierarchical-structure-based sensors.

4. Challenges and Perspectives

Although research on micro-/nanohierarchical structures physically engineered on surfaces is being actively conducted and various potential applications are suggested, some critical limitations (e.g., complex, unstable, expensive, and nonuniform fabrication processes) still hinder the commercialization of hierarchical structures and broadening of their application scope. As discussed in Section 2, structural complexity accompanies the complex combinations of different fabrication processes, whereas commercialization requires low-cost, uniformity, reproducibility, and highly effective production. In addition, many fabrication processes of hierarchical structures rely on the mechanical or chemical instability of substrates (e.g., strain mismatch for wrinkle-based hierarchical structures[42] or resin reflow for micropattern-based hierarchical structures[44]) and are therefore poorly suited for large-area reliable production. For example, micropattern-based hierarchical structures inspired by octopus suction cups were developed using patterned polymeric master molds fabricated through a meniscus-assisted solution-based air-trapping (i.e., partial-wetting) technique.[22] These manufacturing techniques can induce structural instabilities and nonuniformities (i.e., large sample-to-sample variation) during the execution of liquid- and air-trapping processes. Further improvements in sophisticated fabrication processes such as 3D printing and photolithography as well as increases in process reliability using an artificial intelligence would alleviate the difficulties associated with the manufacturing of 3D structures at a micro-/nanoscale.[191] In the case of random-structure-based hierarchical structures, randomness can result in the degradation of sample-to-sample and in-sample uniformity. Alternatively, ordered nanostructures or rationally designed micropatterns can be added as secondary components to improve macroscale uniformity and to add periodicity, although further innovative solutions are required for commercialization.

As another critical limitation, fabrication processes with low design controllability, high technical barriers, and absence of standardization limit the application scope of hierarchical structures. To be applied in various fields, these structures should be easily accessible to researchers via existing standardized processes, and various fit-for-purpose designs should be possible. However, most current processes are often based on the technical know-how of individual laboratories and have poor controllability. For example, in the fabrication of wrinkle-based hierarchical structures, deformation mismatch is induced by applying prestrain to the substrate or subjecting a thermally shrinkable substrate to heat treatment. These deformations cannot be easily controlled and standardized because of their instability and nonuniformity. Therefore, various solutions for increasing controllability and finding standardized processes such as the adoption of rationally designed micropatterns and rationally controllable sacrificial layers have been actively studied to resolve these problems. Moreover, fiber-based hierarchies have limitations, as exemplified by the damage of primary structures during fabrication, high entry barriers of processes such as lithography and chemical vapor deposition used for micro-/nanofiber manufacturing, and difficulty of controlling the tip direction of high-aspect-ratio fibers. Therefore, many researchers have tried to establish solutions such as the use of sacrificial layers for the maintenance of primary structure during fabrication, fabrication process streamlining, and control of nanofiber direction by trapping in micropatterns. Therefore, we expect follow-up research aiming at developing advanced fabrication techniques to allow a more practical utilization of hierarchical structures and to broaden their application scope.

5. Conclusion

This review summarized research on micro-/nanohierarchical structures physically engineered on surfaces and categorized them according to their basic constituent structures. Most of the hierarchical structures are constructed by combining two different structures with different scales or shapes, and each basic structure making up the hierarchical structure can be generally categorized into five groups according to its main function and shape. Rationally designed micropatterns are used to tune mechanical properties or impart the designed surface profile with uniformity, wrinkles provide highly elevated specific surface area or stretchability, fibers are used to increase the active specific surface area, ordered nanopatterns provide surface hydrophobicity/hydrophilicity or structural color, while random structures impart catalytic activity or electrical conductivity. When a hierarchical structure is constructed by combining these basic constituent structures, one of them imparts or dramatically enhances the main function (primary structure), while the others (secondary structures) are combined with the primary structure to support the main function of the primary structure by obtaining synergistic effects. Thereby, hierarchical structures are categorized into four groups according to their primary structure, i.e., rationally designed micropattern-based, wrinkle-based, fiber-based, and random-structure-based hierarchical structures. For each of these types, we summarized their recent research trends and focused on the combinations of different structures with unique functionality and their potential applications (Table 2). For example, a bioinspired hierarchical-structure-based stretchable superomniphobic surface using nanoscale T-shape (primary) and microscale wrinkle (secondary) structures maintained

© 2023 Wiley-VCH GmbH

15214095, 2024, 2, Downloaded from https://onlinelibrary.wiley.com/doi/10.1002/adma.202300871 by Korea Advanced Institute Of, Wiley Online Library on [14/01/2024]. See the Terms and Conditions (https://onlinelibrary.wiley.com/terms-and-conditions) on Wiley Online Library for rules of use; OA articles are governed by the applicable Creative Commons License

their superhydrophobicity regardless of the applied strain.[6] The primary structure helps to achieve high contact angles by controlling the contact area and forming the Cassie–Baxter state required for omniphobicity, while the secondary structure such as the stretchable wrinkle structure helps to maintain the contact angle when pressure or strain is applied. In another example, a heterogeneous adhesive inspired by tree frog's toe pads and the convex cup of octopus suckers was developed.[19] The primary structure of this heterogeneous adhesive is a microscale hexagonal array structure (i.e., a designed micropattern) providing omnidirectional peel resistance and drainage, while the secondary structure is a convex cup structure located on the primary structure (i.e., a designed micropattern), securing strong adhesion under diverse dry and wet conditions.

We also discussed major applications of hierarchical structures, namely functional surfaces with controlled contact angle, dry/wet adhesives, energy-related devices, and physical/chemical/biological sensors. For each application, a proper hierarchical structure is matched in terms of its characteristics and field requirements. In the field of functional surfaces with controlled contact angle, nanostructures have been designed as primary structures to control the contract area and wetting properties and thus regulate the contact angle. Notable examples are superior superomniphobic surfaces based on nanostructures such as nanohoods, nano-T-shapes, nanospears, and nanopillars. In view of their propensity to air gap formation, nanohood arrays can be used to generate Cassie–Baxter states.[1–4] In the field of dry/wet adhesives, the hierarchical structures constructed by combining two different shapes (e.g., engineered surface profiles) are primarily required for adhesion under various dry and wet conditions. For instance, in a gecko-inspired adhesive, the microtip-on-micropillar arrays help to increase van der Waals interactions associated with large specific surface area, the number of hairs (i.e., contact splitting principle),[55] and achieve the effective compliance of the hierarchical structure.[8,9,17] The applications of hierarchical structures in energy harvesting (e.g., TENGs),[58,62,169–177] storage (e.g., battery electrodes),[127,130,178] conversion (e.g., electrolyte membranes of fuel cells),[28,179,180] and self-powered devices[62,181] were also reviewed. The performance of most of these devices is directly related to the effective surface area, i.e., to the physical or chemical contact area. As hierarchical structures physically engineered on surfaces provide high mechanical robustness as well as large specific surface area and roughness, they meet the key requirements of high-performance TENGs. In view of their large reactive surface area, hierarchical structures also hold great promise for physical, chemical, and biological sensors. Specifically, these sensor applications rely on microstructures for constructing the hardware frame in view of their high mechanical stability and rely on nano-/wrinkle structures to enhance sensitivity by increasing the reactive area.[31,33–36]

Overall, despite some limitations, especially those related to complex and nonstandardized processes, active research is being conducted to solve these technical problems. Research on micro-/nanohierarchical structures physically engineered on surfaces has made substantial progress over the past decades. Promising fabrication processes, materials, and structures for improving physicochemical properties are now much better understood, inspiring the development of various functional surfaces and their potential applications. We believe that the present review provides overall research directions and perspectives concerning micro-/nanohierarchical structures physically engineered on surfaces and can guide follow-up research, thus aiding the development of advanced hierarchical structures with more unique and practical properties through the design, fabrication, and analysis of the corresponding unit structures.

Acknowledgements

J.A., H.H., and J.-H.H. contributed equally to this work. This work was supported by a National Research Foundation of Korea (NRF) grant funded by the Korean government (MSIT) (Grant No. 2021R1A2C3008742), the Ministry of Culture, Sports and Tourism and Korea Creative Content Agency (Project Number:R2022020033), and the Development Program of Machinery and Equipment Industrial Technology (Grant No. 20018235, Development of inline nanoimprinter for nanophotonic device) funded by the Ministry of Trade, Industry & Energy (MI, South Korea).

Conflict of Interest

The authors declare no conflict of interest.

Keywords

hierarchical structures, micropatterns, nanopatterns, wrinkles, fibers

Received: January 29, 2023
Revised: April 6, 2023
Published online: November 20, 2023

[1] S. Dong, X. Zhang, Q. Li, C. Liu, T. Ye, J. Liu, H. Xu, X. Zhang, J. Liu, C. Jiang, L. Xue, S. Yang, X. Xiao, *Small* **2020**, *16*, 2000779.
[2] C. Lee, S. Ji, S. Oh, S. Park, Y. Jung, J. Lee, H. Lim, *Nanoscale Adv.* **2022**, *4*, 761.
[3] X. Huang, H. Mutlu, P. Theato, *Adv. Mater. Interfaces* **2020**, *7*, 2000101.
[4] W. Liu, S. Xiang, X. Liu, B. Yang, *ACS Nano* **2020**, *14*, 9166.
[5] W. K. Lee, W. Bin Jung, S. R. Nagel, T. W. Odom, *Nano Lett.* **2016**, *16*, 3774.
[6] G. T. Yun, W. B. Jung, M. S. Oh, G. M. Jang, J. Baek, N. I. Kim, S. G. Im, H. T. Jung, *Sci. Adv.* **2018**, *4*, eaat4978.
[7] C. Greiner, E. Arzt, A. Del Campo, *Adv. Mater.* **2009**, *21*, 479.
[8] Y. Wang, V. Kang, E. Arzt, W. Federle, R. Hensel, *ACS Appl. Mater. Interfaces* **2019**, *11*, 26483.
[9] V. Tinnemann, L. Hernández, S. C. L. Fischer, E. Arzt, R. Bennewitz, R. Hensel, *Adv. Funct. Mater.* **2019**, *29*, 1807713.
[10] H. K. Raut, A. Baji, H. H. Hariri, H. Parveen, G. S. Soh, H. Y. Low, K. L. Wood, *ACS Appl. Mater. Interfaces* **2018**, *10*, 1288.
[11] X. Liu, H. Gu, H. Ding, X. Du, Z. He, L. Sun, J. Liao, P. Xiao, Z. Gu, *Small* **2019**, *15*, 1902360.
[12] Y. Wang, V. Kang, W. Federle, E. Arzt, R. Hensel, *Adv. Mater. Interfaces* **2020**, *7*, 2001269.
[13] L. Xue, B. Sanz, A. Luo, K. T. Turner, X. Wang, D. Tan, R. Zhang, H. Du, M. Steinhart, C. Mijangos, M. Guttmann, M. Kappl, A. Del Campo, *ACS Nano* **2017**, *11*, 9711.
[14] Q. Liu, D. Tan, F. Meng, B. Yang, Z. Shi, X. Wang, Q. Li, C. Nie, S. Liu, L. Xue, *Small* **2021**, *17*, 202005493.
[15] Z. Rong, Y. Zhou, B. Chen, J. Robertson, W. Federle, S. Hofmann, U. Steiner, P. Goldberg-Oppenheimer, *Adv. Mater.* **2014**, *26*, 1456.

 © 2023 Wiley-VCH GmbH

[16] H. Tian, X. Li, J. Shao, C. Wang, Y. Wang, Y. Tian, H. Liu, *Adv. Mater. Interfaces* **2019**, *6*, 1900875.
[17] S. H. Lee, S. W. Kim, B. S. Kang, P. S. Chang, M. K. Kwak, *Soft Matter* **2018**, *14*, 2586.
[18] Y. C. Chen, H. Yang, *ACS Nano* **2017**, *11*, 5332.
[19] D. W. Kim, S. Baik, H. Min, S. Chun, H. J. Lee, K. H. Kim, J. Y. Lee, C. Pang, *Adv. Funct. Mater.* **2019**, *29*, 1807614.
[20] H. Hu, D. Wang, H. Tian, Q. Huang, C. Wang, X. Chen, Y. Gao, X. Li, X. Chen, Z. Zheng, J. Shao, *Adv. Funct. Mater.* **2022**, *32*, 2109076.
[21] L. Zhang, H. Chen, Y. Guo, Y. Wang, Y. Jiang, D. Zhang, L. Ma, J. Luo, L. Jiang, *Adv. Sci.* **2020**, *7*, 2001125.
[22] S. Baik, D. W. Kim, Y. Park, T. J. Lee, S. Ho Bhang, C. Pang, *Nature* **2017**, *546*, 396.
[23] Y. Wang, H. Hu, J. Shao, Y. Ding, *ACS Appl. Mater. Interfaces* **2014**, *6*, 2213.
[24] H. Yi, I. Hwang, J. H. Lee, D. Lee, H. Lim, D. Tahk, M. Sung, W. G. Bae, S. J. Choi, M. K. Kwak, H. E. Jeong, *ACS Appl. Mater. Interfaces* **2014**, *6*, 14590.
[25] J. K. Kim, N. Krishna-Subbaiah, Y. Wu, J. Ko, A. Shiva, M. Sitti, *Adv. Mater.* **2023**, *35*, 2207257.
[26] M. R. Marulli, L. Heepe, S. N. Gorb, M. Paggi, *Mech. Res. Commun.* **2022**, *125*, 103963.
[27] Y. Wang, D. Liu, C. Wang, J. Wu, X. Xu, X. Yang, C. Sun, P. Jiang, X. Wang, *Chem. Eng. J.* **2023**, *457*, 141268.
[28] D. H. Lee, G. T. Yun, G. Doo, S. Yuk, H. Guim, Y. Kim, W. Bin Jung, H. T. Jung, H. T. Kim, *Nano Lett.* **2022**, *22*, 1174.
[29] X. Xia, J. Tu, Y. Zhang, X. Wang, C. Gu, X. B. Zhao, H. J. Fan, *ACS Nano* **2012**, *6*, 5531.
[30] H. Kang, C. Zhao, J. Huang, D. H. Ho, Y. T. Megra, J. W. Suk, J. Sun, Z. L. Wang, Q. Sun, J. H. Cho, *Adv. Funct. Mater.* **2019**, *29*, 1903580.
[31] J. Ji, C. Zhang, S. Yang, Y. Liu, J. Wang, Z. Shi, *ACS Appl. Mater. Interfaces* **2022**, *14*, 24059.
[32] J. Jia, G. Huang, J. Deng, K. Pan, *Nanoscale* **2019**, *11*, 4258.
[33] Y. Yang, S. Duan, W. Xiao, H. Zhao, *Sens. Actuators, A* **2022**, *343*, 113653.
[34] C. Zhang, S. Chen, J. Wang, Z. Shi, L. Du, *Adv. Mater. Interfaces* **2022**, *9*, 2102468.
[35] C. Mahata, H. Algadi, J. Lee, S. Kim, T. Lee, *Measurement* **2020**, *151*, 107095.
[36] J. Jaiswal, P. Singh, R. Chandra, *Sens. Actuators, B* **2021**, *327*, 128862.
[37] M. Chao, Y. Wang, D. Ma, X. Wu, W. Zhang, L. Zhang, P. Wan, *Nano Energy* **2020**, *78*, 105187.
[38] W. G. Bae, H. N. Kim, D. Kim, S. H. Park, H. E. Jeong, K. Y. Suh, *Adv. Mater.* **2014**, *26*, 675.
[39] Q. Chen, N. M. Pugno, *J. Mech. Behav. Biomed. Mater.* **2013**, *19*, 3.
[40] D. Brodoceanu, C. T. Bauer, E. Kroner, E. Arzt, T. Kraus, *Bioinspiration Biomimetics* **2016**, *11*, 051001.
[41] F. J. Martin-Martinez, K. Jin, D. López Barreiro, M. J. Buehler, *ACS Nano* **2018**, *12*, 7425.
[42] W. K. Lee, T. W. Odom, *ACS Nano* **2019**, *13*, 6170.
[43] D. Wang, N. Cheewaruangroj, Y. Li, G. McHale, Y. Jiang, D. Wood, J. S. Biggins, B. Bin Xu, *Adv. Funct. Mater.* **2018**, *28*, 1704228.
[44] J. Choi, W. Jo, S. Y. Lee, Y. S. Jung, S. H. Kim, H. T. Kim, *ACS Nano* **2017**, *11*, 7821.
[45] Z. Chen, X. Lu, H. Wang, J. Chang, D. Wang, W. Wang, S. W. Ng, M. Rong, P. Li, Q. Huang, Z. Gan, J. Zhong, W. Di Li, Z. Zheng, *Adv. Mater.* **2023**, *35*, 2210778.
[46] L. Meng, I. Jeerapan, W. C. Mak, in *Microfluidic Biosensors*, Elsevier, Amsterdam, The Netherlands **2023**, pp. 107–157.
[47] H. Han, Y. S. Oh, S. Cho, H. Park, S. U. Lee, K. Ko, J. M. Park, J. Choi, J. H. Ha, C. Han, Z. Zhao, Z. Liu, Z. Xie, J. S. Lee, W. G. Min, B. J. Lee, J. Koo, D. Y. Choi, M. Je, J. Y. Sun, I. Park, *Small* **2022**, *19*, 2205048.
[48] S. Cho, H. Han, H. Park, S. U. Lee, J. H. Kim, S. W. Jeon, M. Wang, R. Avila, Z. Xi, K. Ko, M. Park, J. Lee, M. Choi, J. S. Lee, W. G. Min, B. J. Lee, S. Lee, J. Choi, J. Gu, J. Park, M. S. Kim, J. Ahn, O. Gul, C. Han, G. Lee, S. Kim, K. Kim, J. Kim, C. M. Kang, J. Koo, et al., *npj Flexible Electron.* **2023**, *7*, 8.
[49] Y. S. Oh, J. H. Kim, Z. Xie, S. Cho, H. Han, S. W. Jeon, M. Park, M. Namkoong, R. Avila, Z. Song, S. U. Lee, K. Ko, J. Lee, J. S. Lee, W. G. Min, B. J. Lee, M. Choi, H. U. Chung, J. Kim, M. Han, J. Koo, Y. S. Choi, S. S. Kwak, S. B. Kim, J. Kim, J. Choi, C. M. Kang, J. U. Kim, K. Kwon, S. M. Won, et al., *Nat. Commun.* **2021**, *12*, 5008.
[50] M. Afshar-Mohajer, X. Yang, R. Long, M. Zou, *Addit. Manuf.* **2023**, *62*, 103368.
[51] W. Zhang, J. Gao, Y. Deng, L. Peng, P. Yi, X. Lai, Z. Lin, *Adv. Funct. Mater.* **2021**, *31*, 2101068.
[52] W. Bin Jung, K. M. Cho, W. K. Lee, T. W. Odom, H. T. Jung, *ACS Appl. Mater. Interfaces* **2018**, *10*, 1347.
[53] W. K. Lee, C. J. Engel, M. D. Huntington, J. Hu, T. W. Odom, *Nano Lett.* **2015**, *15*, 5624.
[54] C. Deng, S. Zhang, H. Wang, G. Zhang, *Nano Energy* **2018**, *49*, 419.
[55] E. Arzt, S. Gorb, R. Spolenak, *Proc. Natl. Acad. Sci. USA* **2003**, *100*, 10603.
[56] S. Schauer, M. Worgull, H. Hölscher, *Soft Matter* **2017**, *13*, 4328.
[57] J. Ahn, J. Gu, Y. Jeong, J.-H. Ha, J. Ko, B. Kang, S. H. Hwang, J. Park, S. Jeon, H. Kim, J.-H. Jeong, I. Park, *ACS Nano* **2023**, *17*, 5935.
[58] G. Jian, Q. Meng, Y. Jiao, F. Meng, Y. Cao, M. Wu, *Nanoscale* **2020**, *12*, 14160.
[59] Y. Xiu, L. Zhu, D. W. Hess, C. P. Wong, *Nano Lett.* **2007**, *7*, 3388.
[60] S. Zhang, Q. Jiang, Y. Xu, C. F. Guo, Z. Wu, *Micromachines* **2020**, *11*, 11070682.
[61] R. Hensel, K. Moh, E. Arzt, *Adv. Funct. Mater.* **2018**, *28*, 1800865.
[62] J. Ahn, Z. J. Zhao, J. Choi, Y. Jeong, S. Hwang, J. Ko, J. Gu, S. Jeon, J. Park, M. Kang, D. V. Del Orbe, I. Cho, H. Kang, M. Bok, J. H. Jeong, I. Park, *Nano Energy* **2021**, *85*, 105978.
[63] M. I. Abid, L. Wang, Q. D. Chen, X. W. Wang, S. Juodkazis, H. B. Sun, *Laser Photonics Rev.* **2017**, *11*, 1600187.
[64] Y. Yang, X. Li, X. Zheng, Z. Chen, Q. Zhou, Y. Chen, *Adv. Mater.* **2018**, *30*, 1704912.
[65] Z. Yao, C. Wang, H. K. Sung, N. Y. Kim, *Mater. Sci. Semicond. Process.* **2014**, *27*, 228.
[66] P. Papadopoulos, B. El Pinchasik, M. Tress, D. Vollmer, M. Kappl, H. J. Butt, *Soft Matter* **2018**, *14*, 7429.
[67] S. J. Woo, J. H. Kong, D. G. Kim, J. M. Kim, *J. Mater. Chem. C* **2014**, *2*, 4415.
[68] P. Nguyen, V. A. Ho, *IEEE Rob. Autom. Lett.* **2019**, *4*, 792.
[69] Z. J. Zhao, S. Hwang, M. Bok, H. Kang, S. Jeon, S. H. Park, J. H. Jeong, *ACS Appl. Mater. Interfaces* **2019**, *11*, 30401.
[70] Z. J. Zhao, J. Ahn, J. Ko, Y. Jeong, M. Bok, S. H. Hwang, H. J. Kang, S. Jeon, J. Choi, I. Park, J. H. Jeong, *ACS Appl. Mater. Interfaces* **2021**, *13*, 3358.
[71] W. Zhang, R. Li, H. Zheng, J. Bao, Y. Tang, K. Zhou, *Adv. Funct. Mater.* **2021**, *31*, 2009057.
[72] M. Yuan, F. Luo, Y. Rao, J. Yu, Z. Wang, H. Li, X. Chen, *Carbon* **2021**, *183*, 128.
[73] G. Zhao, Y. Ling, Y. Su, Z. Chen, C. J. Mathai, O. Emeje, A. Brown, D. Reddy Alla, J. Huang, C. Kim, Q. Chen, X. He, D. Stalla, Y. Xu, Z. Chen, P.-Y. Chen, S. Gangopadhyay, J. Xie, Z. Yan, *Sci. Adv.* **2022**, *25*, abp9734.
[74] Y. Jung, J. Choi, W. Lee, J. S. Ko, I. Park, H. Cho, *Adv. Funct. Mater.* **2022**, *32*, 2201147.
[75] M. Sharifuzzaman, M. A. Zahed, S. Sharma, S. M. S. Rana, A. Chhetry, Y. Do Shin, M. Asaduzzaman, S. Zhang, S. Yoon, X. Hui, H. Yoon, J. Y. Park, *Adv. Funct. Mater.* **2022**, *32*, 202107969.
[76] L. Song, C. Dai, X. Jin, Y. Xiao, Y. Han, Y. Wang, X. Zhang, X. Li, S. Zhang, J. Zhang, Y. Zhao, Z. Zhang, L. Qu, *Adv. Funct. Mater.* **2022**, *32*, 2203270.

© 2023 Wiley-VCH GmbH

15214095, 2024, 2, Downloaded from https://onlinelibrary.wiley.com/doi/10.1002/adma.202300871 by Korea Advanced Institute Of, Wiley Online Library on [14/01/2024]. See the Terms and Conditions (https://onlinelibrary.wiley.com/terms-and-conditions) on Wiley Online Library for rules of use; OA articles are governed by the applicable Creative Commons License

[77] M. Sharifuzzaman, M. A. Zahed, M. S. Reza, M. Asaduzzaman, S. H. Jeong, H. Song, D. K. Kim, S. Zhang, J. Y. Park, *Adv. Funct. Mater.* **2023**, 2208894.
[78] P. Fathi-Hafshejani, J. Orangi, M. Beidaghi, M. Mahjouri-Samani, *Int. J. Extreme Manuf.* **2022**, *4*, 015102
[79] D. Zhang, R. Liu, Z. Li, *Int. J. Extreme Manuf.* **2022**, *4*, 045102
[80] P. Fan, B. Bai, M. Zhong, H. Zhang, J. Long, J. Han, W. Wang, G. Jin, *ACS Nano* **2017**, *11*, 7401.
[81] Z. Wang, Z. Cheng, Y. Zhang, Y. Yu, X. Zhai, Z. Zhao, L. Hu, Y. Hu, *Chem. Eng. J.* **2022**, *429*, 132512.
[82] Y. Xue, W. K. Lee, J. Yuan, T. W. Odom, Y. Huang, *Langmuir* **2018**, *34*, 15749.
[83] W. K. Lee, J. Kang, K. S. Chen, C. J. Engel, W. Bin Jung, D. Rhee, M. C. Hersam, T. W. Odom, *Nano Lett.* **2016**, *16*, 7121.
[84] M. Kato, Y. Kashihara, T. A. Asoh, H. Uyama, *Langmuir* **2020**, *36*, 1467.
[85] S. M. Imani, R. Maclachlan, Y. Chan, A. Shakeri, L. Soleymani, T. F. Didar, *Small* **2020**, *16*, 2004886.
[86] T. Li, K. Hu, X. Ma, W. Zhang, J. Yin, X. Jiang, *Adv. Mater.* **2020**, *32*, 1903266.
[87] J. Baek, W. Bin Jung, Y. Cho, E. Lee, G. T. Yun, S. Y. Cho, H. T. Jung, S. G. Im, *ACS Appl. Mater. Interfaces* **2019**, *11*, 17247.
[88] X. Yang, J. Su, J. Xiong, H. Wang, *Fibers Polym.* **2022**, *23*, 1293.
[89] L. Ladouceur, A. Shakeri, S. Khan, A. R. Rincon, E. Kasapgil, J. I. Weitz, L. Soleymani, T. F. Didar, *ACS Appl. Mater. Interfaces* **2022**, *14*, 3864.
[90] H. Izawa, T. Yonemura, Y. Nakamura, Y. Toyoshima, M. Kawakami, H. Saimoto, S. Ifuku, *Carbohydr. Polym.* **2022**, *284*, 119224.
[91] C. Chen, C. A. Airoldi, C. A. Lugo, R. K. Bay, B. J. Glover, A. J. Crosby, *Adv. Funct. Mater.* **2021**, *31*, 2006256.
[92] J. Rodríguez-Hernández, *Prog. Polym. Sci.* **2015**, *42*, 1.
[93] J. H. Lee, H. W. Ro, R. Huang, P. Lemaillet, T. A. Germer, C. L. Soles, C. M. Stafford, *Nano Lett.* **2012**, *12*, 5995.
[94] Q. H. Thi, L. W. Wong, H. Liu, C. S. Lee, J. Zhao, T. H. Ly, *Nano Lett.* **2020**, *20*, 8420.
[95] G. Lin, P. Chandrasekaran, C. Lv, Q. Zhang, Y. Tang, L. Han, J. Yin, *ACS Appl. Mater. Interfaces* **2017**, *9*, 26510.
[96] T. T. Yu, X. F. Zhang, Y. M. Xu, X. L. Cheng, S. Gao, H. Zhao, L. H. Huo, *Sens. Actuators, B* **2016**, *230*, 706.
[97] K. Wu, H. Z. Yuan, S. J. Li, J. Y. Zhang, G. Liu, J. Sun, *Scr. Mater.* **2019**, *162*, 456.
[98] L. Ma, L. He, Y. Ni, *J. Appl. Phys.* **2020**, *127*, 111101.
[99] S. K. Saha, *Precis. Eng.* **2022**, *76*, 328.
[100] S. Yu, Y. Sun, S. Li, Y. Ni, *Soft Matter* **2018**, *14*, 6745.
[101] M. P. Murphy, S. Kim, M. Sitti, *ACS Appl. Mater. Interfaces* **2009**, *1*, 849.
[102] A. Y. Y. Ho, L. P. Yeo, Y. C. Lam, I. Rodríguez, *ACS Nano* **2011**, *5*, 1897.
[103] W. Chang, W. Li, J. Ma, K. Luo, C. Li, *Langmuir* **2021**, *37*, 8989.
[104] S. H. Cha, H. J. Lee, W. G. Koh, *Biomater. Res.* **2017**, *21*, 1.
[105] M. K. Choi, H. Yoon, K. Lee, K. Shin, *Langmuir* **2011**, *27*, 2132.
[106] S. Hu, H. Jiang, Z. Xia, X. Gao, *ACS Appl. Mater. Interfaces* **2010**, *2*, 2570.
[107] S. Hu, Z. Xia, X. Gao, *ACS Appl. Mater. Interfaces* **2012**, *4*, 1972.
[108] Y. Zhang, C. T. Lin, S. Yang, *Small* **2010**, *6*, 768.
[109] H. E. Jeong, S. H. Lee, P. Kim, K. Y. Suh, *Nano Lett.* **2006**, *6*, 1508.
[110] P. S. Lee, O. J. Lee, S. K. Hwang, S. H. Jung, S. E. Jee, K. H. Lee, *Chem. Mater.* **2005**, *17*, 6181.
[111] H. E. Jeong, J. K. Lee, H. N. Kim, S. H. Moon, K. Y. Suh, *Proc. Natl. Acad. Sci. USA* **2009**, *106*, 5639.
[112] W. Bin Jung, S. Jang, S. Y. Cho, H. J. Jeon, H. T. Jung, *Adv. Mater.* **2020**, *32*, 1907101.
[113] C. Zhu, Z. Qi, V. A. Beck, M. Luneau, J. Lattimer, W. Chen, M. A. Worsley, J. Ye, E. B. Duoss, C. M. Spadaccini, C. M. Friend, J. Biener, *Sci. Adv.* **2018**, *4*, aas9459.
[114] J. Liu, L. Zhang, J. Fan, B. Zhu, J. Yu, *Sens. Actuators, B* **2021**, *331*, 129425.
[115] X. Li, Y. J. Fan, H. Y. Li, J. W. Cao, Y. C. Xiao, Y. Wang, F. Liang, H. L. Wang, Y. Jiang, Z. L. Wang, G. Zhu, *ACS Nano* **2020**, *14*, 9605.
[116] Y. Jung, J. Ahn, J. S. Kim, J. H. Ha, J. Shim, H. Cho, Y. S. Oh, Y. J. Yoon, Y. Nam, I. K. Oh, J. H. Jeong, I. Park, *Small Methods* **2022**, *6*, 2200248.
[117] G. Y. Bae, S. W. Pak, D. Kim, G. Lee, D. H. Kim, Y. Chung, K. Cho, *Adv. Mater.* **2016**, *28*, 5300.
[118] M. Zhang, H. Fan, N. Zhao, H. Peng, X. Ren, W. Wang, H. Li, G. Chen, Y. Zhu, X. Jiang, P. Wu, *Chem. Eng. J.* **2018**, *347*, 291.
[119] S. Gräf, *Adv. Opt. Technol.* **2020**, *9*, 11.
[120] J. Shi, L. Wang, Z. Dai, L. Zhao, M. Du, H. Li, Y. Fang, *Small* **2018**, *14*, 1800819.
[121] K. Kang, J. Park, B. Kim, K. Na, I. Cho, J. Rho, D. Yang, J. Y. Lee, I. Park, *ACS Appl. Mater. Interfaces* **2020**, *12*, 39024.
[122] Y. R. Kim, M. P. Kim, J. Park, Y. Lee, S. K. Ghosh, J. Kim, D. Kang, H. Ko, *ACS Appl. Mater. Interfaces* **2020**, *12*, 58403.
[123] B. Zhu, Y. Ling, L. W. Yap, M. Yang, F. Lin, S. Gong, Y. Wang, T. An, Y. Zhao, W. Cheng, *ACS Appl. Mater. Interfaces* **2019**, *11*, 29014.
[124] J. Shao, Y. Ding, W. Wang, X. Mei, H. Zhai, H. Tian, X. Li, B. Liu, *Small* **2014**, *10*, 2595.
[125] Q. Tian, W. Yan, T. Chen, D. Ho, *J. Mater. Chem. C* **2021**, *9*, 17129.
[126] T. Saison, C. Peroz, V. Chauveau, S. Berthier, E. Sondergard, H. Arribart, *Bioinspiration Biomimetics* **2008**, *3*, 046004.
[127] L. Cong, H. Xie, J. Li, *Adv. Energy Mater.* **2017**, *7*, 1601906.
[128] F. Chen, X. Cui, C. Liu, B. Cui, S. Dou, J. Xu, S. Liu, *Sci. China Mater.* **2021**, *64*, 852.
[129] L. Feng, K. Y. Wang, J. Powell, H. C. Zhou, *Matter* **2019**, *1*, 801.
[130] G. S. Dos Reis, H. P. de Oliveira, S. H. Larsson, M. Thyrel, E. C. Lima, *Nanomaterials* **2021**, *11*, 424.
[131] C. Karaman, O. Karaman, N. Atar, M. L. Yola, *Microchim. Acta* **2022**, *189*, 24.
[132] Y. Liu, J. Chen, B. Cui, P. Yin, C. Zhang, *C* **2018**, *4*, 53.
[133] Z. Xie, H. Wang, M. Li, Y. Tian, Q. Deng, R. Chen, X. Zhu, Q. Liao, *Chem. Eng. J.* **2022**, *435*, 135025.
[134] L. Wang, S. Huang, Q. Y. Li, L. Y. Ma, C. Zhang, F. Liu, M. Jiang, X. Yu, L. Xu, *Chem. Eng. J.* **2022**, *435*, 134762.
[135] W. Wang, P. F. Li, R. Xie, X. J. Ju, Z. Liu, L. Y. Chu, *Adv. Mater.* **2022**, *34*, 2107877.
[136] E. Huovinen, J. Hirvi, M. Suvanto, T. A. Pakkanen, *Langmuir* **2012**, *28*, 14747.
[137] M. F. Wang, N. Raghunathan, B. Ziaie, *Langmuir* **2007**, *23*, 2300.
[138] H. B. Jo, J. Choi, K. J. Byeon, H. J. Choi, H. Lee, *Microelectron. Eng.* **2014**, *116*, 51.
[139] M. Zhou, X. Xiong, B. Jiang, C. Weng, *Appl. Surf. Sci.* **2018**, *427*, 854.
[140] Y. Zhang, Q. Xing, A. Chen, M. Li, G. Qin, J. Zhang, C. Lei, *Chem. Eng. Sci.* **2022**, *262*, 118027.
[141] S. S. Latthe, C. Terashima, K. Nakata, A. Fujishima, *Molecules* **2014**, *19*, 4256.
[142] A. Marmur, *Langmuir* **2004**, *20*, 3517.
[143] Y. T. Cheng, D. E. Rodak, *Appl. Phys. Lett.* **2005**, *86*, 144101.
[144] Z. J. Wei, W. L. Liu, D. Tian, C. L. Xiao, X. Q. Wang, *Appl. Surf. Sci.* **2010**, *256*, 3972.
[145] Z. Chen, Z. Zhang, *Water Sci. Technol.* **2020**, *82*, 207.
[146] R. Sun, J. Zhao, C. Liu, N. Yu, J. Mo, Y. Pan, D. Luo, *Prog. Org. Coat.* **2022**, *171*, 107016.
[147] R. M. Do Nascimento, C. Cottin-Bizonne, C. Pirat, S. M. M. Ramos, *Langmuir* **2016**, *32*, 2005.
[148] C. Rin Yu, A. Shanmugasundaram, D. W. Lee, *Appl. Surf. Sci.* **2022**, *583*, 152500.

© 2023 Wiley-VCH GmbH

15214095, 2024, 2, Downloaded from https://onlinelibrary.wiley.com/doi/10.1002/adma.202300871 by Korea Advanced Institute Of, Wiley Online Library on [14/01/2024]. See the Terms and Conditions (https://onlinelibrary.wiley.com/terms-and-conditions) on Wiley Online Library for rules of use; OA articles are governed by the applicable Creative Commons License

[149] A. B. D. Cassie, S. Baxter, *Trans. Faraday Soc.* **1944**, *40*, 546.
[150] J. Yeo, D. S. Kim, *Microsyst. Technol.* **2010**, *16*, 1457.
[151] M. K. Kim, W. Yao, Y. R. Cho, *Colloids Surf., A* **2022**, *634*, 127973.
[152] Y. Lai, Y. Tang, J. Gong, D. Gong, L. Chi, C. Lin, Z. Chen, *J. Mater. Chem.* **2012**, *22*, 7420.
[153] Z. Sun, T. Liao, K. Liu, L. Jiang, J. H. Kim, S. X. Dou, *Small* **2014**, *10*, 3001.
[154] L. Zheng, K. Wang, D. Hou, X. Jia, Z. Zhao, *Desalination* **2022**, *526*, 115512.
[155] M. H. Abd Aziz, M. H. D. Othman, J. R. Tavares, M. A. B. Pauzan, M. Tenjimbayashi, A. W. Lun, N. H. Alias, A. F. Ismail, M. A Rahman, J. Jaafar, *Appl. Surf. Sci.* **2022**, *598*, 153702.
[156] W. Zhang, Y. Li, J. Liu, B. Li, S. Wang, *J. Membr. Sci.* **2017**, *535*, 258.
[157] W. Li, Q. Yu, H. Yao, Y. Zhu, P. D. Topham, K. Yue, L. Ren, L. Wang, *Acta Biomater.* **2019**, *92*, 60.
[158] M. Seth, S. Jana, *NanoWorld J.* **2020**, *6*, 26.
[159] Z. Jin, H. Mei, L. Pan, H. Liu, L. Cheng, *ACS Sustainable Chem. Eng.* **2021**, *9*, 4111.
[160] B. Bhushan, Y. C. Jung, K. Koch, *Langmuir* **2009**, *25*, 3240.
[161] H. Tian, H. Liu, J. Shao, S. Li, X. Li, X. Chen, *Soft Matter* **2020**, *16*, 5599.
[162] X. Li, P. Bai, X. Li, L. Li, Y. Li, H. Lu, L. Ma, Y. Meng, Y. Tian, *Friction* **2022**, *10*, 1192.
[163] S. Wang, H. Luo, C. Linghu, J. Song, *Adv. Funct. Mater.* **2021**, *31*, 2009217.
[164] M. Wall, "Gecko Feet Inspire Climbing Space Robots," www.space.com/30258-nasa-gecko-space-robot-sticky-feet.html (accessed: August 2022).
[165] Y. Chen, J. Meng, Z. Gu, X. Wan, L. Jiang, S. Wang, *Adv. Funct. Mater.* **2020**, *30*, 1905287.
[166] K. Autumn, Y. A. Liang, S. T. Hsieh, W. Zesch, W. P. Chan, T. W. Kenny, R. Fearing, R. J. Full, *Nature* **2000**, *405*, 681.
[167] F. Tramacere, N. M. Pugno, M. J. Kuba, B. Mazzolai, *Interface Focus* **2015**, *5*, 20140050.
[168] W. J. P. Barnes, *Science* **2007**, *318*, 203.
[169] Y. Zou, J. Xu, K. Chen, J. Chen, *Adv. Mater. Technol.* **2021**, *6*, 200916.
[170] Q. Zhou, K. Lee, K. N. Kim, J. G. Park, J. Pan, J. Bae, J. M. Baik, T. Kim, *Nano Energy* **2019**, *57*, 903.
[171] H. Lee, H. E. Lee, H. S. Wang, S. M. Kang, D. Lee, Y. H. Kim, J. H. Shin, Y. W. Lim, K. J. Lee, B. S. Bae, *Adv. Funct. Mater.* **2020**, *30*, 2005610.
[172] Z. Zheng, J. Xia, B. Wang, Y. Guo, *Nano Energy* **2022**, *95*, 107047.
[173] H. Cho, J. Chung, G. Shin, J. Y. Sim, D. S. Kim, S. Lee, W. Hwang, *Nano Energy* **2019**, *56*, 56.
[174] D. Jang, Y. Kim, T. Y. Kim, K. Koh, U. Jeong, J. Cho, *Nano Energy* **2016**, *20*, 283.
[175] X. Chen, J. Xiong, K. Parida, M. Guo, C. Wang, C. Wang, X. Li, J. Shao, P. S. Lee, *Nano Energy* **2019**, *64*, 103904.
[176] J. Wang, K. Wang, Z. Qiu, Y. Liu, R. Chen, C. Wu, J. Lin, *Energy Technol.* **2021**, *9*, 2100571.
[177] S. Jin, Y. Wang, M. Motlag, S. Gao, J. Xu, Q. Nian, W. Wu, G. J. Cheng, *Adv. Mater.* **2018**, *30*, 1705840.
[178] X. Peng, Z. Taie, J. Liu, Y. Zhang, X. Peng, Y. N. Regmi, J. C. Fornaciari, C. Capuano, D. Binny, N. N. Kariuki, D. J. Myers, M. C. Scott, A. Z. Weber, N. Danilovic, *Energy Environ. Sci.* **2020**, *13*, 4872.
[179] H. Cho, S. Moon Kim, Y. Sik Kang, J. Kim, S. Jang, M. Kim, H. Park, J. Won Bang, S. Seo, K. Y. Suh, Y. E. Sung, M. Choi, *Nat. Commun.* **2015**, *6*, 8484.
[180] M. Abbaszadeh Amirdehi, S. Saem, M. P. Zarabadi, J. M. Moran-Mirabal, J. Greener, *Adv. Mater. Interfaces* **2018**, *5*, 1800290.
[181] Y. Wang, H. Wu, L. Xu, H. Zhang, Y. Yang, Z. L. Wang, *Sci. Adv.* **2020**, *6*, eabb9083.
[182] J. Ahn, J. S. Kim, Y. Jeong, S. Hwang, H. Yoo, Y. Jeong, J. Gu, M. Mahato, J. Ko, S. Jeon, J. H. Ha, H. S. Seo, J. Choi, M. Kang, C. Han, Y. Cho, C. H. Lee, J. H. Jeong, I. K. Oh, I. Park, *Adv. Energy Mater.* **2022**, *12*, 2201341.
[183] X. Li, Y. Zhang, Y. Cheng, X. Chen, W. Tan, *Ceram. Int.* **2021**, *47*, 9214.
[184] X. Sun, C. Gao, L. Zhang, M. Yan, J. Yu, S. Ge, *Sens. Actuators, B* **2017**, *251*, 1.
[185] Q. Wang, X. Kou, C. Liu, L. Zhao, T. Lin, F. Liu, X. Yang, J. Lin, G. Lu, *J. Colloid Interface Sci.* **2018**, *513*, 760.
[186] J. Ahn, J. Ha, Y. Jeong, Y. Jung, J. Choi, J. Gu, S. H. Hwang, M. Kang, J. Ko, S. Cho, H. Han, K. Kang, J. Park, S. Jeon, J. Jeong, I. Park, *Nat. Commun.* **2023**, *14*, 833.
[187] A. Garg, E. Mejia, W. Nam, M. Nie, W. Wang, P. Vikesland, W. Zhou, *Small* **2022**, *18*, 202106887.
[188] M. Dabrowski, M. Cieplak, P. S. Sharma, P. Borowicz, K. Noworyta, W. Lisowski, F. D'Souza, A. Kuhn, W. Kutner, *Biosens. Bioelectron.* **2017**, *94*, 155.
[189] S. Yang, C. Zhang, J. Ji, Y. Liu, J. Wang, Z. Shi, *Adv. Mater. Technol.* **2022**, *7*, 2200309.
[190] J. Zhou, X. Long, J. Huang, C. Jiang, F. Zhuo, C. Guo, H. Li, Y. Q. Fu, H. Duan, *npj Flexible Electron.* **2022**, *6*, 55.
[191] Z. Zhu, D. W. H. Ng, H. S. Park, M. C. McAlpine, *Nat. Rev. Mater.* **2021**, *6*, 27.
[192] H. Zhang, M. Zhou, H. Zhao, Y. Lei, *Nanotechnology* **2021**, *32*, 502006.



Junseong Ahn is a Postdoctoral Researcher at the Korea Institute of Machinery & Materials. He received his BS, M.S., and Ph.D. degrees from the Hanyang University (2017), KAIST (2019), and KAIST (2023), respectively. His current research interest is focused on micro-/nanostructuring and their application to sensors and energy-harvesting devices.

© 2023 Wiley-VCH GmbH

15214095, 2024, 2, Downloaded from https://onlinelibrary.wiley.com/doi/10.1002/adma.202300871 by Korea Advanced Institute Of, Wiley Online Library on [14/01/2024]. See the Terms and Conditions (https://onlinelibrary.wiley.com/terms-and-conditions) on Wiley Online Library for rules of use; OA articles are governed by the applicable Creative Commons License



Hyeonseok Han is currently a Ph.D. candidate at the Korea Advanced Institute of Science and Technology, Daejeon, South Korea. He received his BS and M.S. degrees from the Hanyang University, Ansan, South Korea, in 2015 and the Pohang University of Science and Technology, Pohang, South Korea, in 2020, respectively. His research interests lie in wearable devices and micro-/nanofabrication for biomedical applications.



Ji-Hwan Ha is currently a Ph.D. candidate at the Korea Advanced Institute of Science and Technology, Daejeon, South Korea. He received his BS and M.S. degrees from the Soongsil University, Seoul, South Korea, in 2018 and in 2020, respectively. His current research interest is focused on micro-/nanofiber fabrication and their application to biosensors and medical devices.



Jun-Ho Jeong is a Principal Researcher at the Korea Institute of Machinery & Materials. He is also a Faculty Member of the Department of Nano-Mechatronics at the University of Science and Technology. He received his BS, M.S., and Ph.D. from the Hanyang University (1990), KAIST (1993), and KAIST (1998), respectively, all in mechanical engineering. His research interests are nanoimprinting, nanofabrication, holograms, microneedles, and drug delivery.



Inkyu Park received his B.S., M.S., and Ph.D. from KAIST (1998), the University of Illinois at Urbana-Champaign (2003), and the University of California at Berkeley (2007), respectively, all in mechanical engineering. He has been with KAIST since 2009 and is currently a KAIST Endowed Chair Professor at KAIST. His research interests are nanofabrication, smart sensors for healthcare, environmental and biomedical monitoring, nanomaterial-based sensors and wearable electronics. He has published more than 160 international journal articles and 200 international conference papers, and holds more than 40 registered domestic and international patents in the area of micro-electro-mechanical-systems (MEMS) and nanoengineering.

© 2023 Wiley-VCH GmbH

15214095, 2024, 2, Downloaded from https://onlinelibrary.wiley.com/doi/10.1002/adma.202300871 by Korea Advanced Institute Of, Wiley Online Library on [14/01/2024]. See the Terms and Conditions (https://onlinelibrary.wiley.com/terms-and-conditions) on Wiley Online Library for rules of use; OA articles are governed by the applicable Creative Commons License